MSc Thesis

Numerical analysis of mesoscale air transport within a squall line

supervisors:
Leo Kroon
Gert-Jan Steeneveld

author:
Mike Budde

June 8, 2017

Abstract

The mesoscale air transport within a squall line was (quantitatively) studied, using a high resolution simulation of 600m. Additionally, an 3km simulation was performed. The mesoscale Weather Research and Forecasting (WRF) model was used for these simulations. To make the transport of air visible, a passive tracer was used in the model. The simulation was performed for a squall line that moved over western Europe at 12th of July 2010. Validation analysis showed that the simulation is reasonably well in accordance with observations. The passive tracer was released in three layers (0-2km, 2-4km and 4-6km) to show the transport between these different layers, towards other layers and towards the top of the atmosphere. The differences between the two simulations were relative small for the regions of downdrafts. The cold pool was very similar between the simulations as well. This study showed that an increase in horizontal resolution will lead to slightly more transport of air towards higher altitudes. However, the main pattern of mixing of air within a squall line remains the same.

Table of contents

1 Introduction

Mesoscale convective systems (MCS) can be sorted into different categories. One of these categories is squall lines. A squall line is a mesoscale convective system which is organised linearly. The exact definition of a MCS differs among studies. The American Meteorological Society's Glossary of Meteorology defined a MCS as a thunderstorm which is able to produce continuous precipitation over a horizontal length scale in the order of 100km or larger and whereby the influence of Coriolis acceleration becomes significant for the development of those thunderstorms (Brey & Geer, 2000). A squall line is often called a type 2 MCS, this means that the storm is driven by the effects of a cold pool (Markowski & Richardson, 2010). These systems are characterised by updrafts of air and areas with stratiform and convective precipitation (Houze, 2004). At the location of the mature cell, convective precipitation can be found, while the stratiform precipitation is located at the rear of the squall line (Figure 1).

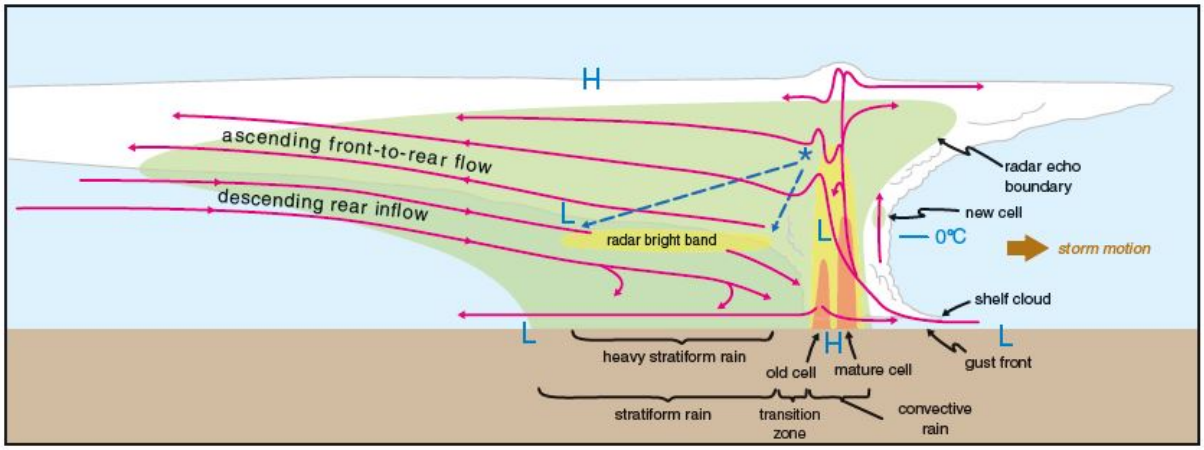

Figure 1: *Vertical cross section of a conceptual model of a squall line. The green area indicates the location where radar echo can be found. The yellow and orange bands show the location of more intense regions of radar echo. The pink lines represent the most important air flow paths. (From Markowski & Richardson (2010), adapted from Houze (1989))*

A widely used theory in the understanding of squall lines, is the theory of Rotunno et al. (1988), also known as the Rotunno-Klemp-Weisman (RKW) theory. This theory states that the optimal conditions for the development of a squall line will be reached when the cold pool intensity and the wind shear in the lower atmosphere are in balance. This theory was revised by Weisman & Rotunno (2004) (See Appendix A). Figure 2 illustrates the three stages of a convective system that are described by this theory. In the first stage (a), the updraft leans downshear due to the absence of a cold pool, so $C \ll \Delta U$, where C represents the theoretical speed of movement of a two-dimensional gravity wave (Benjamin, 1968), in this case the cold pool, and ΔU represents the vertical wind shear perpendicular to the squall line in the lower atmosphere. In the second stage (b) the updraft is standing upright, this is due to the balance between C and ΔU ($C \approx \Delta U$). In the third stage (c) the cold pool becomes stronger than the wind shear ($C \gg \Delta U$) resulting in an updraft tilted in the upshear direction. There is some criticism on this theory, for example Stensrud et al. (2005) showed that intense, long lived, squall lines often not only have a wind shear in the lower atmosphere but in the deeper layers as well. A more extensive overview of the RKW theory, revision and criticism will be given in Appendix A.

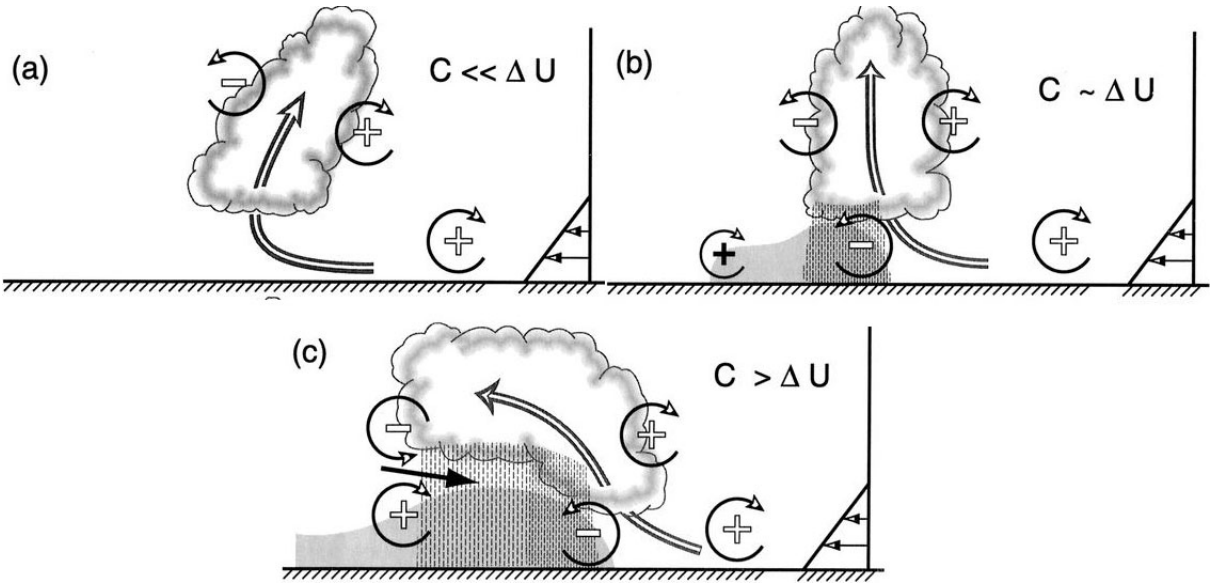

Figure 2: *Illustration of the three stages of a convective system according the RKW theory. The thick double line represents the updraft. The cold pool is displayed as a light grey area, the rain is represented by vertical lines, more dense lines means more intense precipitation The black solid line shows the rear inflow current. The vorticity is shown by the circular arrows and the wind shear perpendicular to the squall line (ΔU) is shown on the bottom right corner of each image. C represents the theoretical speed of movement of a two-dimensional gravity wave (From Weisman & Rotunno (2004))*

Nowadays research is mostly focussed on the influences of horizontal and vertical resolution on the intensity (eg. precipitation rate and wind speed) of a squall line in numerical models. Bryan & Morrison (2012) showed that a horizontal resolution of 250m gives the most realistic results. They also concluded that the influence of horizontal resolution on the intensity of a squall line is larger than changes in parametrization schemes. Lebo & Morrison (2015) looked at the influences of the horizontal resolution on the mixing of air inside a squall line. They concluded that horizontal resolutions coarser than 500m suppress the entrainment and detrainment of air. Both studies used a 3D numerical weather prediction model to simulate an idealised squall line. This means that they simplified the physics of the model, to be able able to discard a large part of the uncertainties with regard to atmospheric phenomena. Uebel & Bott (2015) looked at a real case squall line, but they used a lower horizontal resolution (2,8km). Although they got fairly good results of mixing in a squall line, they also concluded that convection is not completely solved in the 2.8km horizontal resolution simulation.

It is widely known that computational power increases relatively fast. This will result in a possibility to increase the resolution of operational meteorological models. An increase in resolution may result in the situation that parametrization will be (partly) solved in a model. One of these parametrizations is the Cumulus parametrization. According to Skamarock et al. (2008) this parametrizations is not needed any more with resolutions of 10km or higher. However this parametrization is widely used in studies with resolutions higher than 10km (Bélair & Mailhot, 2001; Petch et al., 2002; Bryan et al., 2003; Litta & Mohanty, 2008; Dawson et al., 2010; Hong et al., 2010; Yu & LEE, 2010; Kukkonen et al., 2012; Pimonsree et al., 2016). For the exact understanding of this cumulus parametrization and also to determine to what extend high resolution models (partly) solve these parametrization, a better understanding of the vertical transport of air masses and dynamical entrainment is needed (de Rooy et al., 2013).

The aim of this study is to get a better (quantitative) insight in the behaviour of the mixing of air within a squall line. We will extend the study of Uebel & Bott (2015), by increasing the horizontal resolution to 600m in a WRF modelling experiment. The findings of this research will be compared with the findings of Uebel & Bott (2015). To reach this aim, the following

research questions will be answered.

- What is the influence of increasing horizontal model resolution on mixing of air in a squall line?
    1. What are the changes in the size of updrafts and downdrafts with changing horizontal resolution?
    2. What are the changes in the strength of updrafts and downdrafts with changing horizontal resolution?
    3. What are the changes in strength and location of the cold pool with changing horizontal resolution?

In the next chapter, the methodology can be found. In chapter 3, a short validation analysis of the model output as well as an overview of the results will be given. Chapter 4 consists of Discussion and recommendations. This thesis will end with the conclusions in chapter 5.

2 Methodology

In this chapter a case description an overview of the numerical set-up, and the research set-up will be given, respectively.

2.1 Case description

In the period of 10 - 14 July 2010, the weather in western Europe was dominated by severe thunderstorms. During this period a mid-level trough was located over the North Atlantic Ocean (Figure 3). There was a weak low pressure system just to the south of Ireland. The combination of this trough and the low pressure system resulted in a flow from Spain towards the North. This situation happens more often over western Europe and is referred to as the "Spanish Plume" (Carlson & Ludlam, 1968). A more detailed overview of a Spanish Plume is given in Appendix A.

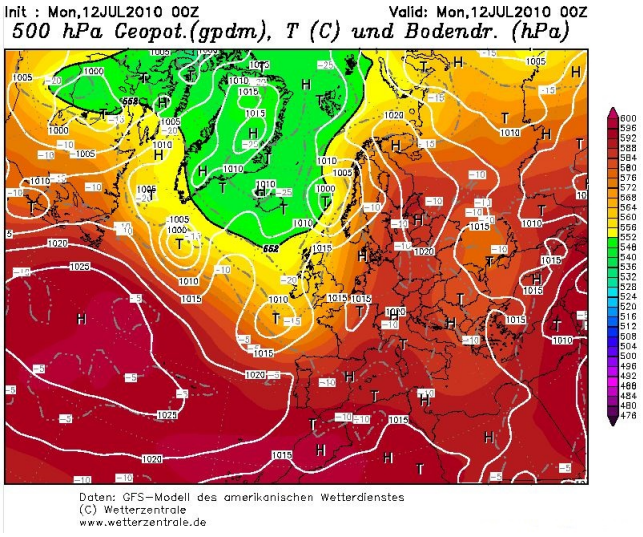

Figure 3: *500hPa geopotential height in dam (colours) and the pressure at surface in hPa (solid white lines) at 12-07-2010 00UTC from the GFS analysis (From* Wetterzentrale *(2010)).*.

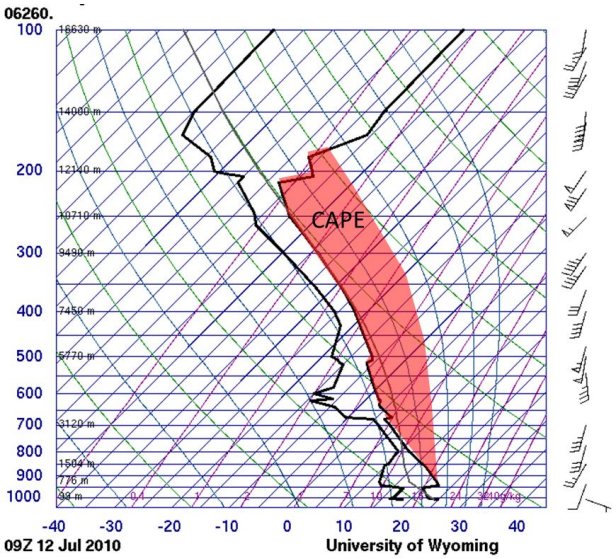

Figure 4: *Sounding of De Bilt at 09UTC, 12-07-2010. The line on the left represents dew point (° C) and the line on the right hand side is the temperature(° C). The red area shows the amount of CAPE (From* University of Wyoming *(2010)).*

In the evening of the 11th of July 2010, some small showers were moving from the Pyrenees into the southern part of France. At that moment, high Convective Available Potential Energy (CAPE) values, up to 2600 J/kg, have been observed. This is one of the drivers which resulted in an intensification of the showers from 00UTC, 12th of July, and onwards. After some hours these small showers merged with a line of convective thunderstorms over central France, which formed large MCS (Figure 5). This system continued to intensify during the morning. In the regions ahead of the squall line a relatively large low level wind shear was found. For example in De Bilt at 00 UTC a wind speed of 5kts was measured at the surface, at 800m the wind speed was 10kts, at 1500m it was already 25kts and this increased to 35kts at 3000m height Figure 4). Therefore one of the important ingredients for the development of a squall line, wind shear, was clearly present in this region. At 06 UTC, 12th of July, the northern part of the MCS, now is organised as a squall line, reached the border between France and Belgium. While moving over the Ardennes, the squall line gets partly fractured. Over the Netherlands some showers developed ahead of the squall line, which soon merged with the squall line. During this period

the orientation of the squall line changed from West-East towards a more South-North direction. In the same time, the squall line extended towards the south. The squall line intensified until it reached Denmark around 14 UTC, 12th of July. After 14 UTC it weakened again due to a decrease in CAPE and a lack of vertical wind shear in this area. Precipitation of more than 40mm in 24h was measured in a large part in the north-east of The Netherlands on the 12th of July 2012, with a maximum of 45.8mm in Eelde. Wind gusts of 100km/h and higher were observed in the eastern parts of the Netherlands (*KNMI: Maximum wind gust* (2010)). Some of these strong wind gusts caused material damage in that area. (Hut, 2010).

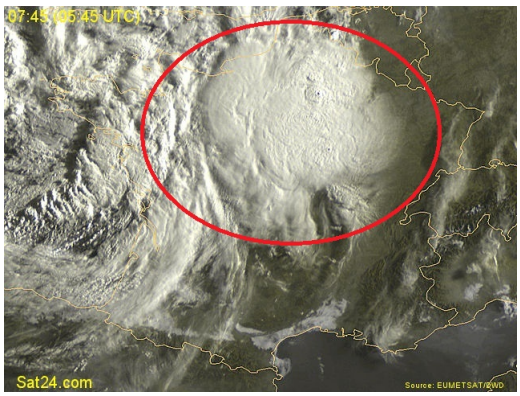

Figure 5: *Satellite image (visible channel) of a large MCS above France at 05:45 UTC at 12th of July 2010. The circle indicates the location of the large MCS (From SAT24).*

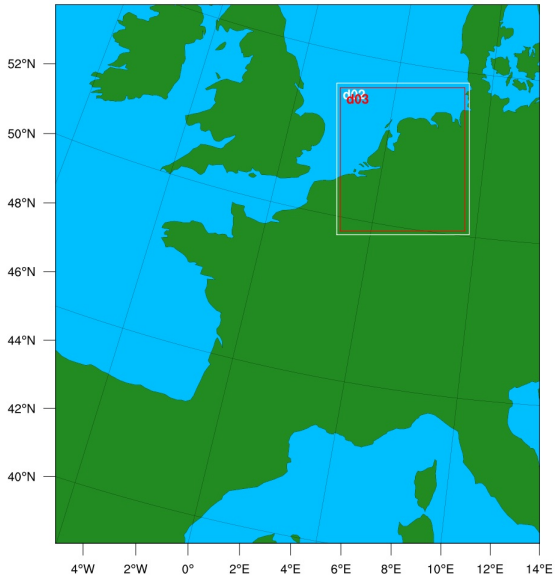

Figure 6: *The three different domains used in this study. The white square and red square represent the second and third domain, respectively.*

2.2 Numerical Set-up

The numerical model simulation was performed using the mesoscale Weather Research and Forecasting (WRF) model (Skamarock et al., 2008). The model set-up was similar to the set-up of Uebel & Bott (2015). However, in this study a higher resolution simulation has been performed as well. The model consists of three domains with two nested domains. A large domain is needed to catch the developing phase of the disturbance that developed into the squall line. This developing phase was needed in the model to obtain a more realistic simulation of the squall line. Because of limitations in computation power, it was not possible to run the complete domain on a fine resolution, therefore nested domains were used. The outer domain includes a large part of southern and western Europe, reaching from Spain to northern Germany. The inner domains cover almost incidental areas and are located at the same place (Figure 6). This gave the opportunity to analyse the influence of the resolution only. In an ideal situation, the two inner domains, would be located exactly on top of each other. However, that was technically impossible as WRF needs a minimum of five grid points between two nested domains to be able to interpolate the relatively coarse values to a higher resolution. In the end ten grid points were located between the two nested domains, because the model was unstable when using five grid points. These two domains only include Belgium, The Netherlands, and the western part of Germany (Figure 6). An overview of the resolution and the amount of grid points of the nested domains can be found in Table 1.

Table 1: *Grids used in the three domains.*

Domain	Horizontal resolution (km)	Grid points X	Grid points Y
1	9	180	200
2	3	175	169
3	0.6	776	746

Parametrization was needed to define the sub-grid scale processes. Therefore different parametrization schemes have been used in this model. An overview of the parametrization schemes can be found in Table 2. For the details of the schemes, see Skamarock et al. (2008).

Table 2: *Parametrization schemes used in the simulations.*

Physical option	Parametrization scheme
Microphysics	WSM6 scheme
Cumulus physics	Kain-Fritsch scheme
Longwave radiation	Rapid Radiative Transfer Model (RRTM)
Shortwave radiation	MM5 (Dudhia) Shortwave
Land-surface model	Noah Scheme
Planetary Boundary	Yonsei University (YSU) Scheme

2.3 Experiment Set-up

The experiment can be divided in three parts. In the first part a sensitivity analysis has been done to evaluate the WRF performance (Section 2.3.1). After this, the simulations were evaluated by a model performance validation (Section 2.3.2). Finally a passive tracer experiment was performed(Section 2.3.3), which gave a quantitative insight of the air transport within a squall line.

2.3.1 Sensitivity Analysis

The main goal of the sensitivity analysis was to get a model run which was able to simulate the main features of the squall line. The influence of parametrization schemes on the results should be small (Bryan & Morrison, 2012). In this study the main focus was on the differences in spin-up time, i.e. the start of the simulation. It appeared that the start time of the simulation has a large influence on the representation of the squall line in WRF. Simulations with an early start and a spin-up time of six hours or more, had some problems with simulating the squall line. Some of the early simulations did not have a squall line at all (e.g. the first simulation, shown in Figure 7A)). The results improved drastically when no spin-up time was used, as a clear squall line was formed in the output (Figure 7B). This improvement is probably due to the fact that the disturbance is already in the ECMWF-data which is was used as initialisation of the model at the starting time step. The most realistic run was found with a starting time at 00 UTC at the 12th of July 2010. This model simulation was used for further analysis.

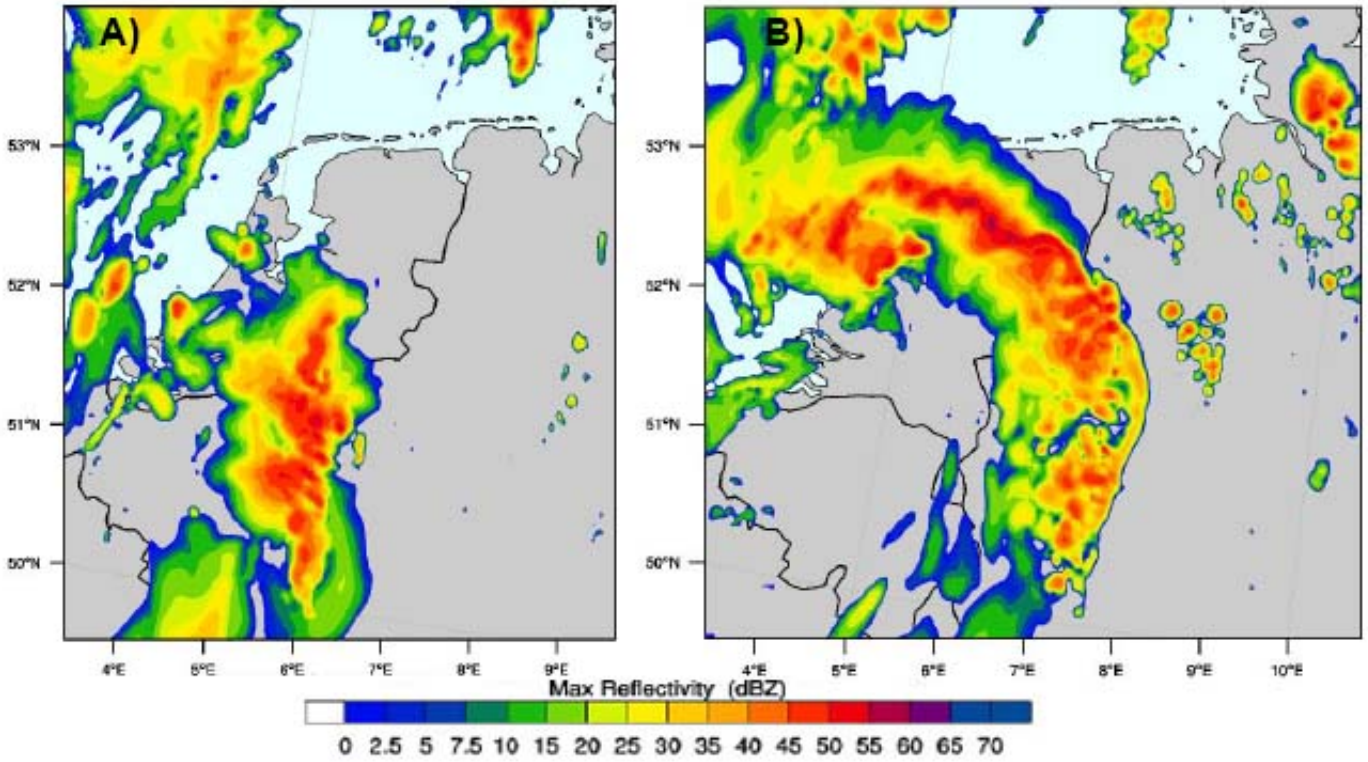

Figure 7: *Maximum reflectivity at 12 UTC of the first simulation (A), with 6 hour spin-up time and of the simulation without spin-up time (B), which is used for the actual analysis in the results chapter. Both are showing the second domain, with a resolution of 3km.*

2.3.2 Validation

To asses of the performance of the simulation a validation assessment was performed. This validation firstly focussed on spatial differences, and secondly on time series of multiple parameters at various meteorological stations. In the first part precipitation radar images were compared with simulated radar reflectivity. As the exact amount of precipitation is not relevant for this study, a comparison of radar reflectivity with precipitation rates is satisfying as reflectivity data are converted radar reflectivity values. The most important factor are the shape of the squall line and the locations of the most intense precipitation areas, i.e. high reflectivity values. Besides radar reflectivity, satellite observations have been compared with model output as well. As WRF did not have a standard way to represent clouds, outgoing long wave radiation at the top of the atmosphere was used to compare the model results with the satellite observations. By this a clear representation of the high and mid level clouds can be obtained. However, is excludes low clouds. As there is no better alternative, this is a reasonable product to compare with satellite observations.

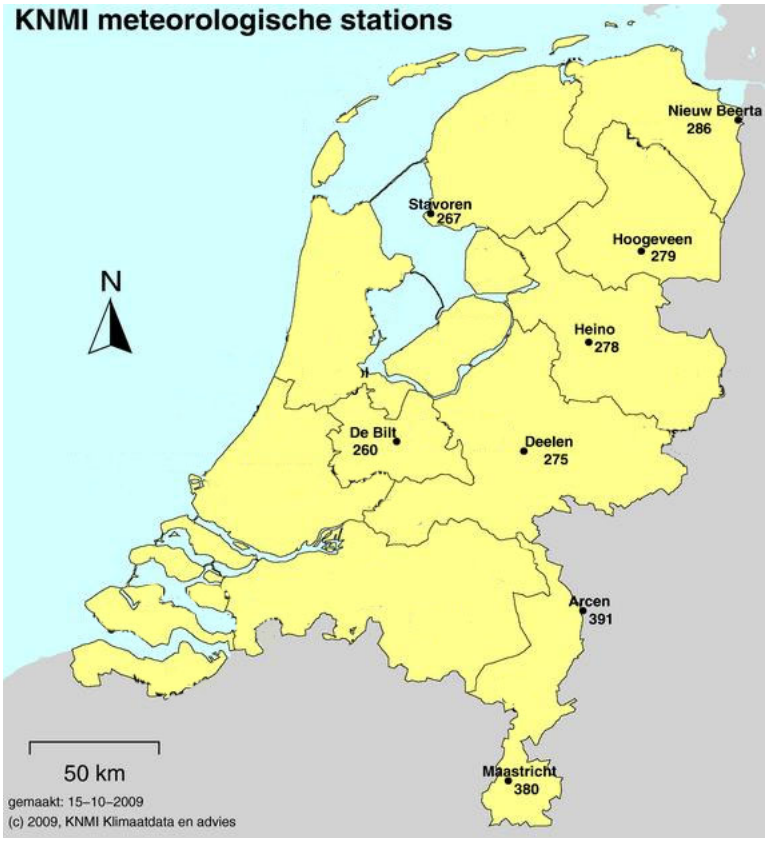

Figure 8: *The eight KNMI stations, name and station number, used for validation of the model results.*

The second part of the validation focussed on time series of different parameters at various meteorological stations. In total 8 Dutch meteorological stations were selected (Figure 8). As the strongest part of the squall line moved over the eastern part of the Netherlands, most of the selected stations are located in this area. Time series of temperature, wind speed and surface pressure were made. These time series give a clear overview of the timing and intensity of the squall line at the different stations. Besides these time series, also the Root Mean Square Error (RMSE),

$$RMSE = \sqrt{\frac{1}{n} * \sum_{i=1}^{N} (P_i - O_i)^2} \tag{1}$$

and the Mean Bias Error (MBE),

$$MBE = \frac{1}{n} * \sum_{i=1}^{N} (P_i - O_i) \tag{2}$$

of the model results were calculated for temperature and wind speed. Where P_i are the modelled values and O_i are the observation values. The RMSE is more sensitive for outliers than the MBE. These two parameters give a good overview of the model performance (Willmott, 1982).

2.3.3 Passive tracer analysis

The passive tracer experiment consists of two simulations. The 3km and the 0.6km resolution simulation (Table 1), hereafter referred to as coarse and fine resolution simulation, respectively. The coarse resolution is comparable to the resolution used by Uebel & Bott (2015) (2.8km).

This simulation consisted of 50 vertical layers with a thickness of 20m near the surface increasing to 1km at 22km height. Almost half of all the levels was located in the first 2km height. This is comparable with the vertical grid of Uebel & Bott (2015). The fine resolution simulation had slightly different settings. With the same settings as the coarse resolution simulation, the model became unstable. therefore some additions had to be made; the top of the atmosphere is raised from 30hPa to 10hPa. To keep the same distribution of the vertical levels in the lower part of the atmosphere, 20 new levels were added at the top of the atmosphere.

For this tracer experiment, a new option for passive tracers had to be built in WRF. This tracer was introduced to quantify the vertical air flows within the squall line. These air flows are a key process for the cumulus convection (de Rooy et al., 2013). The tracer showed the amount and origin of air within the squall line, this gave a better insight in the heterogeneity of up and downdrafts as well as the origin of air within the cold pool. An overview of the additions made to WRF to get the tracer working is given in Appendix A. For the tracer experiment three different passive tracers were introduced in the model. Thesy all had an initial mixing ratio of 1. The tracers were released on the same heights as in Uebel & Bott (2015). The first tracer was released in the layer between the surface and 2km height, the second between 2 and 4km and the third between 4 and 6km height, called TR_low, TR_mid and TR_high, respectively. In both simulations, the tracers were released at 11 UTC on the 12th of July, because at that moment the squall line is well visible and is located in the middle of the domain. This gives enough time to analyse the squall line before it moves out of the domain. The tracer was released in front of the squall line with an initial mixing ratio of 1. By releasing the tracer directly in front of the squall line, no differences in mixing ratio can develop due to processes ahead of the squall line.

The analysis will focus on the influence of horizontal model resolution on the updraft size and downdraft size, their strength and the strength and location of the cold pool. To analyse this, vertical cross sections of the tracer mixing ratios have been made. These vertical cross sections were well suitable to analyse the size of the updraft and downdrafts. Besides the vertical cross sections, horizontal cross sections were analysed to determine what influences these updrafts and downdrafts had on the precipitation. After this, the strength and location of the cold pool were analysed. To finalize a short comparison of the results with the RKW-theory was made.

3 Results

This chapter consists of two parts. A validation of the model results and the results to answer the research questions.

3.1 Model validation

This section consists of two parts. The focus on the first part will be on the spatial validation of the model, which is mostly done visually. In the second part the focus will be on the validation of the timing, using different observations of stations.

3.1.1 Spatial validation

Although the goal is not to create exactly the same squall line in the model as observed, it is important to have a reasonable and realistic squall line. To get a realistic run, a small sensitivity analysis was performed. The squall line is located over the north-eastern part of the Netherlands at 11 UTC, 12th of July, according the observations (Figure 9). This radar image differs slightly from the radar image used in Uebel & Bott (2015), they did not have precipitation precipitation data for a large area behind the squall line. This difference is caused by the use of different precipitation radars. Our study included, additionally to the German radar, the Dutch precipitation radars because these had a better coverage of the area behind the squall line. In the radar image a clear straight line can be found, it extends from the south-western part of Germany to the north-east of the Netherlands. The northern part of the squall is clearly weaker than the other parts. The spatially averaged precipitation rate is lower (2-10 mm/h) in this weak part than in the strong parts (10-100 mm/h). In the weak part more separated cells instead of one continues line of heavy precipitation (>10 mm/h) were simulated. Taking a closer look at this radar image, a second band of high precipitation can be found. This band is probably formed at the cold front. This means that the squall line is in front of the cold front, a so-called prefrontal squall line.

Comparing the observed radar reflectivity (Figure 9) with the reflectivity of the simulation (Figure 10), The simulation has a delay of about one hour, this did not caused problems in answering the research questions. The simulated squall line is still located over the central part of the Netherlands, whereas in the observations, the squall line already reached the northern part of the Netherlands. Although the orientation of the squall line is a bit different than the observations, it shows a clear line of increased reflectivity and some scattered cells towards the north. The band of increased precipitation behind the squall line can be found in the reflectivity too (Figure 10), however it is not as clear as in the observations. Looking at the simulation of Uebel & Bott (2015) and our simulation, their simulation is located even more to the south than in our simulation (Figure 10 & 11). However their orientation of the squall line looks slightly better.

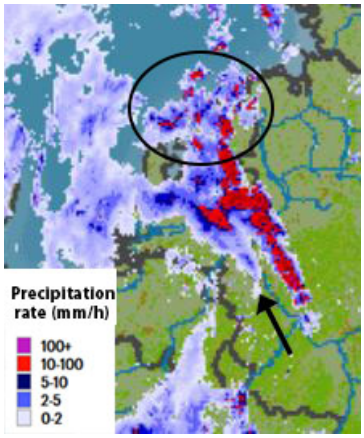

Figure 9: *Precipitation radar image at 11 UTC, 12th of July 2010. The black circle shows the location of the weak part of the squall line. The arrow shows the second band of increased precipitation (From: http://www.meteox.com, Adapted).*

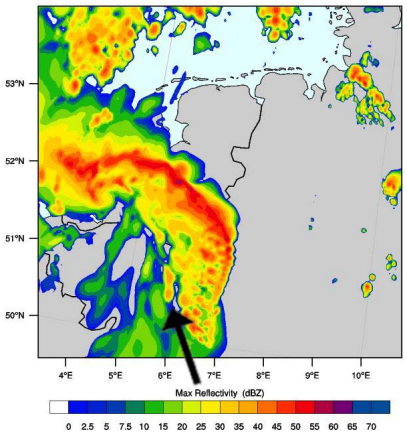

Figure 10: *Maximum reflectivity (dbZ) of the simulation at 11 UTC, 12th of July 2010. The arrow shows the second band of increased reflectivity.*

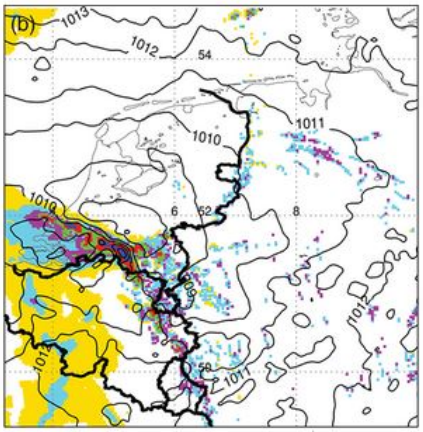

Figure 11: *Simulated precipitation rate with surface pressure (hPa) at 11 UTC (From Uebel & Bott (2015))*

In Figure 12 and 13 we compare the simulation with a satellite observation. Unfortunately, WRF is not able to simulate clouds integrated over all the layers. Therefore a substitute infrared image was created as a substitute, using the outgoing longwave radiation (Figure 13). In the simulation the cloud band is slightly more southerly at 11 UTC. The simulation does not show the clear spots over Belgium. However the simulation shows some convective clouds in front of the squall line, over the Wadden Sea, which are present in the satellite image as well. Moreover, the simulations shows some thinner clouds to the north of North Holland, which are also visible in the satellite image as well. Furthermore, the model is well capable of simulating the sharp increase in cloudiness over the east of the Netherlands.

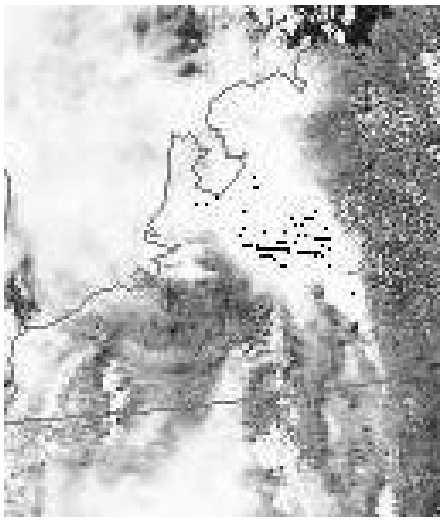

Figure 12: *Visible satellite image (841-867nm) of the MODIS satellite, taken at 10.51 UTC. (From: http://www.sat.dundee.ac.uk)*

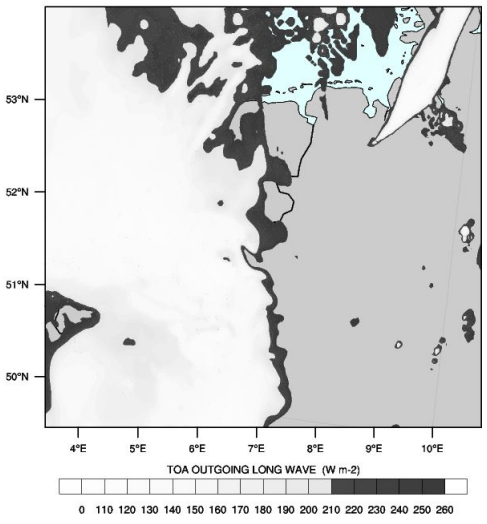

Figure 13: *Long wave radiation (Wm^{-2}) at the top of the atmosphere at 11 UTC.*

To conclude, the simulation is not perfect. However, it is does a reasonable job in simulating the squall line. The model is able to simulate the main features of the squall line and shows a

strong squall line which moves in the same direction as the real squall line. The orientation of the squall line is reasonable as well. Therefore, the spatial validity of the simulation should not create problems in answering the research questions.

3.1.2 Temporal validation

In general, the model performs well before the passage of the squall line (Figure 14). As described above, the model has some problems to simulate the exact timing, and intensity of the temperature drop during the passage. However, the simulation was very good for the meteorological station of Arcen. The simulated temperature almost exactly follows the observations until the passage of the disturbance. At 9 UTC the squall line moves over Arcen, with the result of a temperature drop of 9°C (From 28°C to 19°C). The value of the temperature drop is almost perfect. The only difference is that the drop is too fast, this means that the temperature gradient is higher in the simulation. After the drop the temperature increases again, but again the change of temperature is too fast in the simulation. At the moment of the drop (9 UTC) and the rise (11 UTC) of the temperature, a strong increase in wind speed up to 9 m/s is observed. In the observations the increase in wind speed is less pronounced, with a maximum of 4 m/s. This jump in temperature and wind speed is accompanied by a small temporal increase in simulated pressure (not shown). This increase in pressure shows the location of the mesohigh and therewith the location of the cold pool. Unfortunately there are hardly any observations of pressure for July 2010 at the KNMI-stations, thus this change in pressure cannot be validated.

For the station De Bilt, the model has more problems to simulate the observations well. In the morning of a sunny day, one would expect an increase in temperature, this is also observed in De Bilt. However,in the simulation (Figure 14), the temperature stays around the 20 °C until 10 UTC, where after a small temperature increase is simulated. Between 10 UTC and 14 UTC, the temperature simulation is reasonable. However, after 14 UTC, the simulation deviates again from the observations. Thus the temperature simulation does not perform very well for De Bilt. On the other hand, wind speed is simulated quite well. The simulated wind speed is in general close to the observed wind speed. However, At 9 UTC the model calculates a wind speed which is too high, 8 m/s instead of 3 m/s.

The model results for Nieuw Beerta shows a different pattern, before the passage of the squall line the model simulates a temperature which is too low (Figure 14). At 9 UTC, the observed temperature starts to decrease sooner than the simulated temperature. This is due to scattered rain showers which are located on the northern part of the squall line. In the simulation, these scattered rain showers are located more northward (Figure 9), which will not move over Nieuw Beerta. Therefore, the model estimates a longer temperature rise. At the moment of the passage of the squall line, the temperature in the simulation suddenly drops by 8 °C . After the passage on 12UTC, the simulation performs well. The simulation is reasonable until 15 UTC, where after the observations are showing an increase in wind speed while the simulations shows a small decrease in the wind speed.

Looking at the statistics for these three stations (Table 3), it becomes clear that the simulation of temperature at De Bilt is not done very well. While the best simulation of wind speed can be found at De Bilt. This agrees with the results found above. The previous paragraph showed that temperature and wind speed at simulated well for both Arcen and Nieuw Beerta. However, the statistics still show a relatively large error, this can be explained by the limited amount of data points (18).

To conclude, the model performs reasonably well in simulating the main features. There are some problems with the intensity and timing but this will not create any problems with answering the research question.

Table 3: *Mean Bias Error (MBE) and Root Mean Square Error (RSME) of the simulated temperature and wind speed relative to observations.*

	2m Temperature (°C)		10m Wind Speed (m/s)	
Station name	MBE	RMSE	MBE	RMSE
Arcen	-0.96	4.07	1.27	5.38
De Bilt	-2.77	11.73	0.69	2.93
Nieuw Beerta	-0.46	1.97	-1.19	5.07

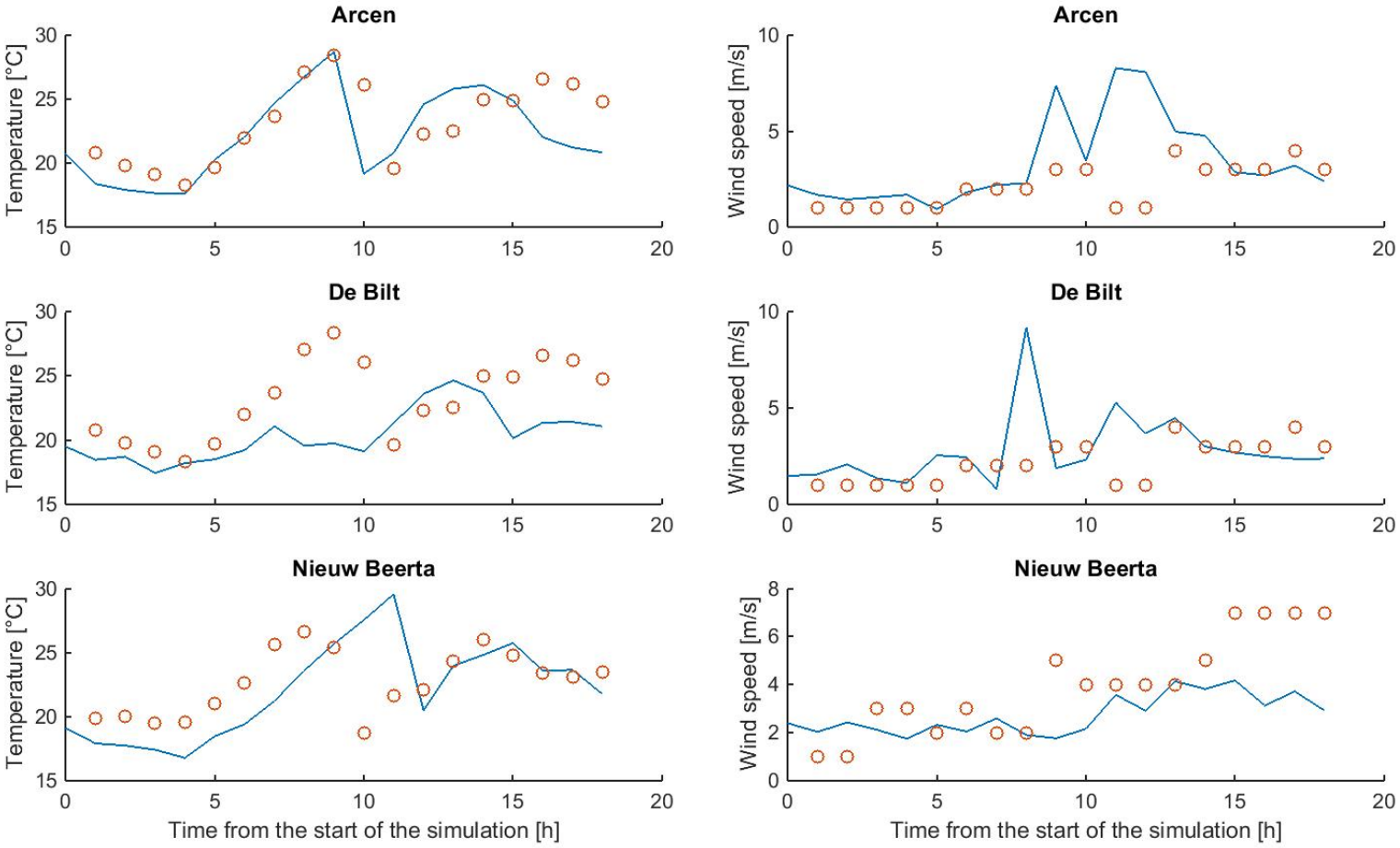

Figure 14: *Observations (red dots) and simulated (blue line) 2m temperature (° C) on te left hand side, on the right hand side the observation against the simulated 10m wind speed (m/s).)*

3.2 Passive tracer Analysis

In the next section the results of the Passive tracer Analysis are presented. In the first section the analysis focusses on the tracer mixing ratios. In the second section the focus is on the cold pool and instability. This chapter ends with a short comparison of the results with the RKW theory.

3.2.1 Tracer mixing ratios

This section focusses on the updraft and downdrafts of air. The location of all the cross-sections which are shown in Figure 15. The first half hour after the initialisation of the squall line an interesting shape can be seen in the vertical cross section (Figure 16). Both the coarse and fine resolution show barely a displacement of the tracer at the surface. However, around 1km height a sudden jump is seen. This shift is caused by an inversion about 1 km height (not shown).

At the top of the inversion, the wind speed increases from 25kt to 65kt (not shown). This increase in wind speed causes the tracer above 1km to move faster along the wind than the tracer below 1km. At the same time, a small part of TR_low is transported to higher altitudes up to 3km and 4.5km for the coarse and fine resolution simulations, respectively. Besides the differences in height, it is clear that in the coarser resolution simulation, the updraft of the tracer is wider and mixing ratio is lower than in the fine resolution simulation. This upward transport is caused by a relatively strong vertical wind at a 6°longitude. The vertical wind speed in the fine resolution simulation is stronger than in the low simulation run at 11.30 UTC (not shown), this explains the difference in upward transport of the tracer between the two different simulations.

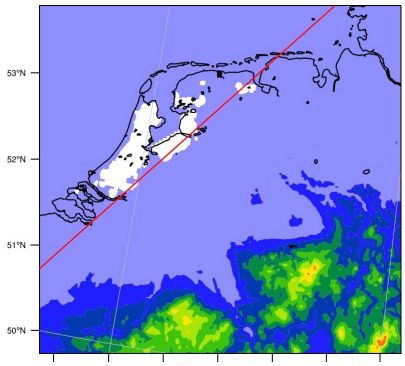

Figure 15: *Elevation map of the coarse resolution domain. The red line shows the location of the vertical cross-sections.*

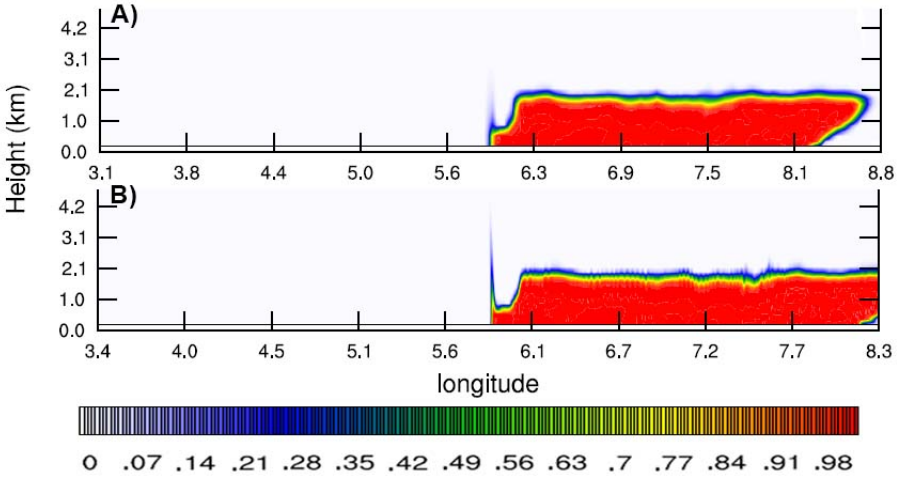

Figure 16: *Vertical cross-sections with the mixing ratio of Tr_low at the coarse (A) and fine (B) resolution simulation at 1130 UTC. The location of this cross-section can be found in Figure 15.*

One hour after the initialisation, almost nothing happened with the TR_high (Figure 17). This tracer is transported eastward, but it is still not transported to different altitudes. However, TR_low and TR_mid are transported upwards. For TR_low, the tracer in both the fine and coarse resolution is transported up to a height of 13.6km (Figure 17). The main differences can be found between 6.1°-6.5°longitude. Where the coarse resolution simulation shows a smooth upward transport with mixing ratios up to 0.75, approximately, the fine resolution simulation gives a less smooth pattern in mixing ratios, with mixing ratios up to 1.This means that in the coarse run 75% and in the fine run 100% of the air at that location comes from the lower 2km of the atmosphere. TR_mid shows a similar pattern, the coarse simulation has again a smoother pattern with slightly lower mixing ratios then the fine resolution simulation. Thus the finer resolution leads to smaller but stronger up- and downdrafts. The vertical wind speed confirms this.

For the coarse simulation, the maximum vertical wind speed exceeds 7.5 m/s over almost the whole height of the troposphere in one narrow line (Figure 18). The troposphere is located at about 12km height for both simulations. At this height the temperature does not drop

with height any more. The maximum vertical wind speed in the fine resolution is tilted. The strongest region of vertical wind speed near the surface can be found at 7.3°longitude. At 10km height this location has a strong negative vertical wind speed. The maximum wind speed is located slightly westward. The overall pattern in the fine resolution is a lot more spiky than in the coarse simulation. The most striking feature in Figure 18 is the downward winds. The coarse simulation shows wind speeds up to 3m/s while for the fine resolution the wind speed exceed 6m/s. This is probably the reason why the tracer has such a spiky appearance between 6.1°-6.5°longitude. The tracer is mainly transported upward in the coarse resolution simulation. In the high resolution simulation it is first transported upward and then it comes in an area with downward wind and will it is transported downward. Hereafter it reaches an area with upward winds, and is transported up again. This up- and downward movement continues, creating the spiky pattern.

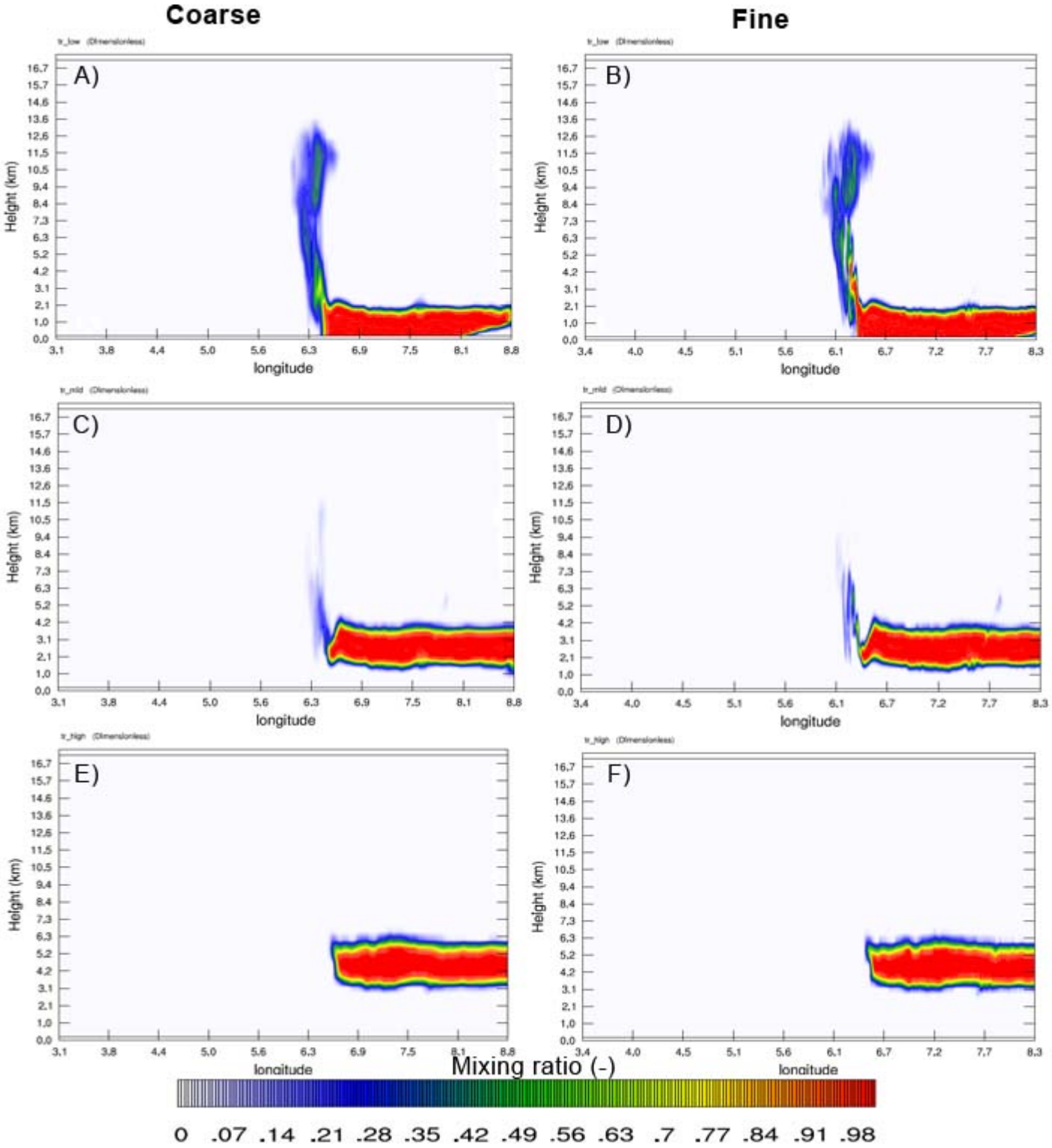

Figure 17: *Vertical cross sections with the mixing ratio of Tr_low (A,B), TR_mid(C,D) and TR_high(E,F) at 12 UTC, 12th of July 2010. The left column shows the figures from the coarse resolution simulation and the right column shows the results of the fine resolution runs. The location of this cross-section can be found in Figure 15.*

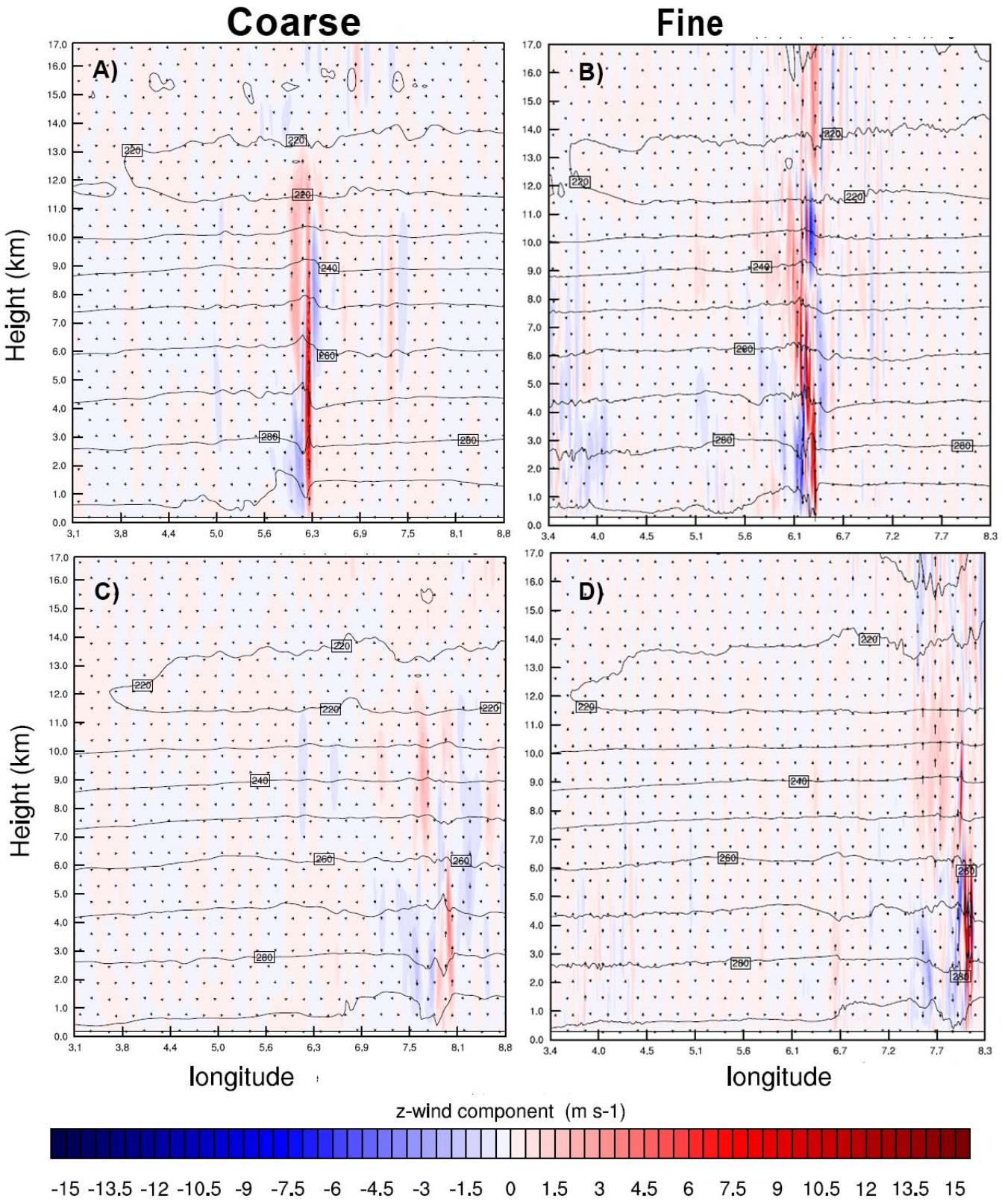

Figure 18: *Vertical wind speed (m/s) (shaded), wind direction (arrows) and temperature (°C) (black contours) of the coarse simulation (A,C) and of the fine simulation (B,D) at 12 UTC (A,B) and 14 UTC (C,D) at the same cross-section as in Figure 15.*

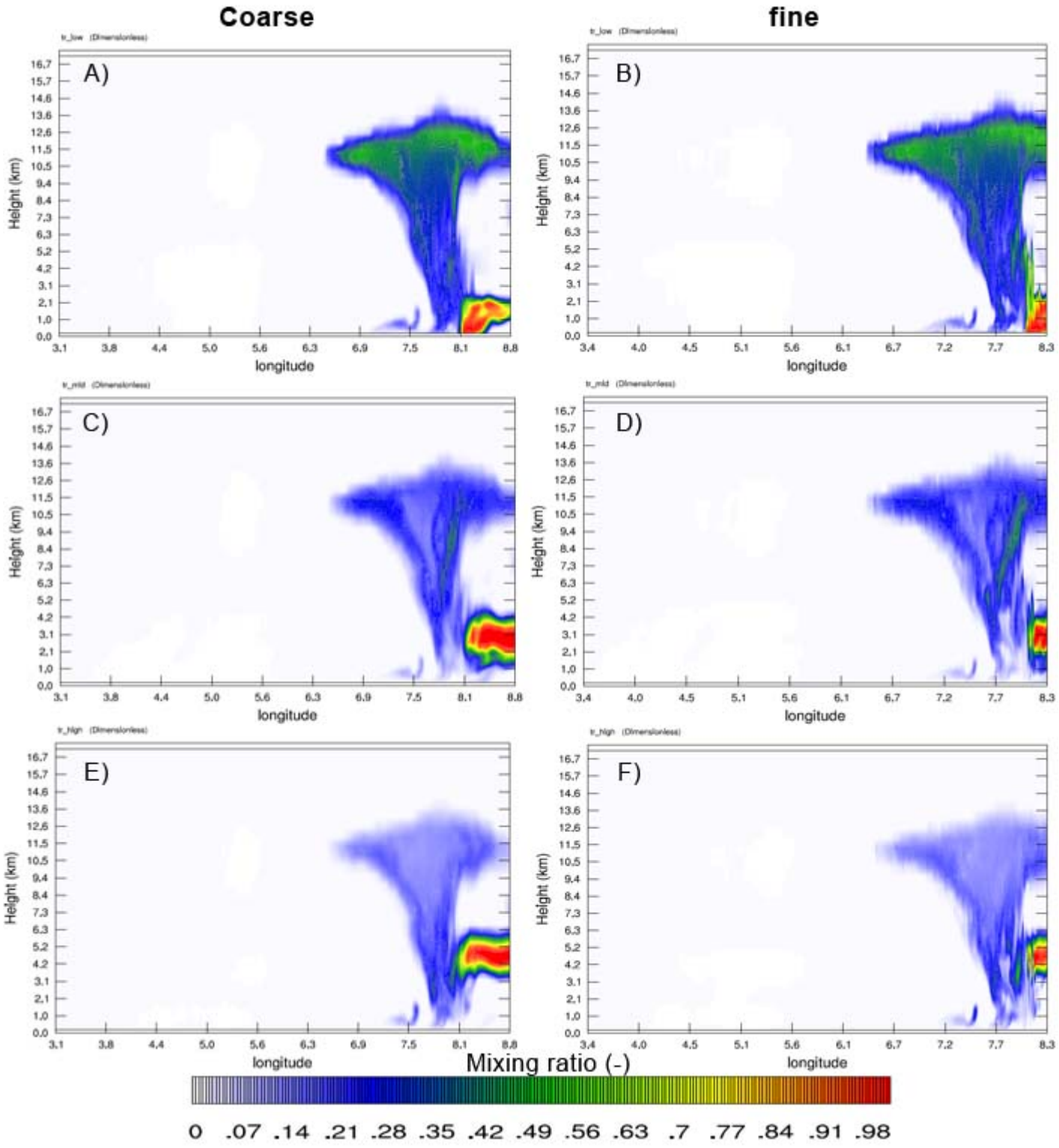

Figure 19: *Vertical cross sections with the mixing ratio of Tr_low (A,B), TR_mid(C,D) and TR_high(E,F) at 14 UTC, 12th of July 2010. The left column shows the figures from the coarse resolution simulation and the right column shows the results of the fine resolution runs. The location of this cross-section can be found in Figure 15.*

Three hours after the initialisation, all the tracers have been partly transported upward up to the troposphere (about 14km) and partly transported downward (Figure 19). Especially TR_low is transported to other altitudes with mixing ratios up to 0.58 while TR_mid and Tr_high have mixing ratios up to 0.37 and 0.18, respectively. The figures of the coarse resolution simulation look very similar to the fine resolution simulation. The same clear pattern as at 12 UTC is faced. The coarse resolution simulations shows a more smooth transport with slightly lower mixing ratios at the locations with the maximum mixing ratios.

The vertical wind speed at 14 UTC has weakened for the coarse simulation(Figure 18) compared to 12 UTC. The minimum and maximum vertical wind speed are -2.5 m/s and 4 m/s, respectively. In the high resolution a shallow but very strong updraft is seen with vertical wind speed up to 15 m/s. This causes a new input of Tr_low into the higher parts of the atmosphere, which can be seen in the fine simulation of Figure 19 at 8 °longitude.

At Eta-level 36, at approximately 11.5km height, the largest area of TR_low is found. The horizontal cross section shows a clear difference between the coarse and fine resolution simulation (Figure 20). The area of mixing ratios higher than 0.1 is more extensive in the finer simulation than in the coarser simulation. Where the highest amount of grid cells have a mixing ratio of about 0.1 (3.3%) in the coarse resolution simulation, the fine resolutions shows the highest amount of grid cells have a mixing ratio of about 0.5 (3.4%) (Figure 21). Thus it is clear that according to the fine simulation, more air is transported upward from the lowest part of the troposphere towards the highest part of the troposphere. This is explained by the vertical wind speed. For a vertical wind speed smaller than 10m/s, there are no differences between the coarse and fine simulation (not shown). However, looking at vertical wind speed with values exceeding 10m/s, it is clear that the fine resolution calculates more grid cells with this vertical wind speed (Figure 21). This higher amount of grid cells with a strong upward vertical wind speed are able to transport more of the tracers from the lower part of the atmosphere towards 11.5km height.

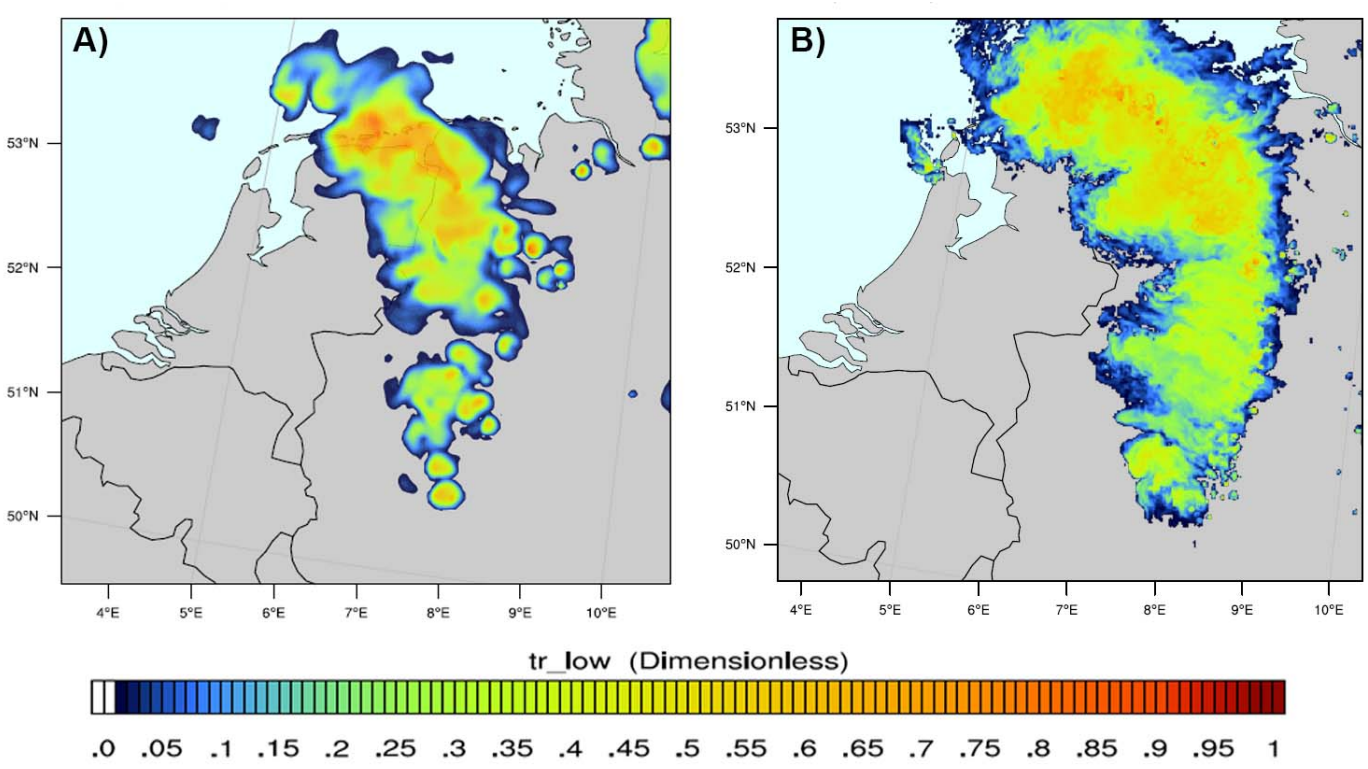

Figure 20: *Horizontal cross-section of the mixing ratio TR_low at Eta-level 36 (approximately 11.5km height) at 14UTC. Coarse resolution (A) and fine resolution (B).*

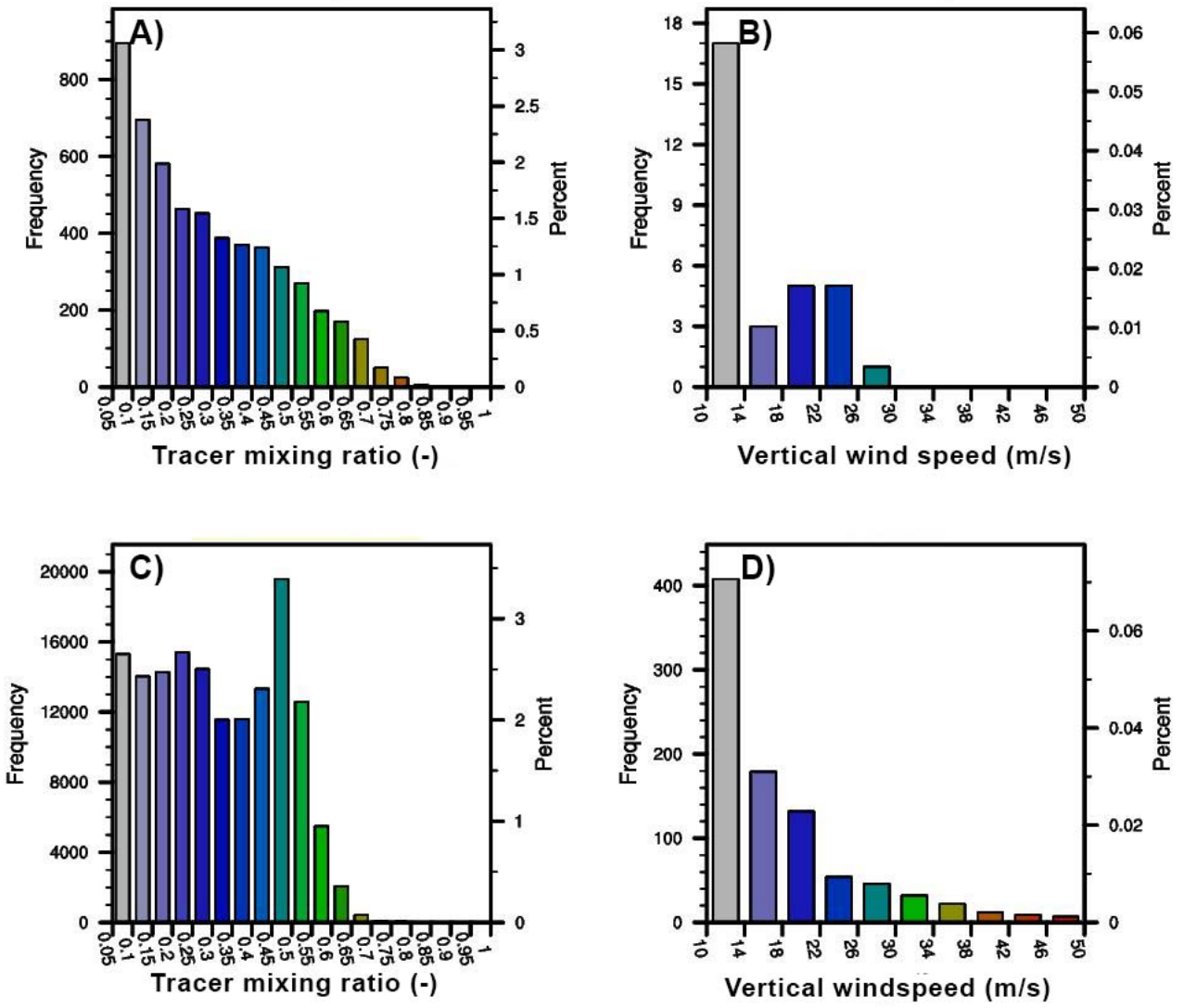

Figure 21: *Histogram of the mixing ratios (A,C) and the vertical wind speed (m/s) (B,D) in the horizontal cross-section given in Figure 20. The scales of the y-axes differ due to the different amount of grid points in the coarse and fine simulation, and the removal of values below the threshold of 0.05 and 10m/s for the tracer mixing ratio and vertical wind speed, respectively.*

Stronger and narrower updrafts within a squall line will results in smaller and more intense convective precipitation at the location of the updrafts (Johnson & Hamilton, 1988). This is shown in the reflectivity data, which is a good proxy for precipitation The fine resolution simulation has a larger area with relatively high reflectivity mainly due to an increase in relatively small patches with higher reflectivity (Figure 22). This means that the model calculates more precipitation for the fine resolution simulation.

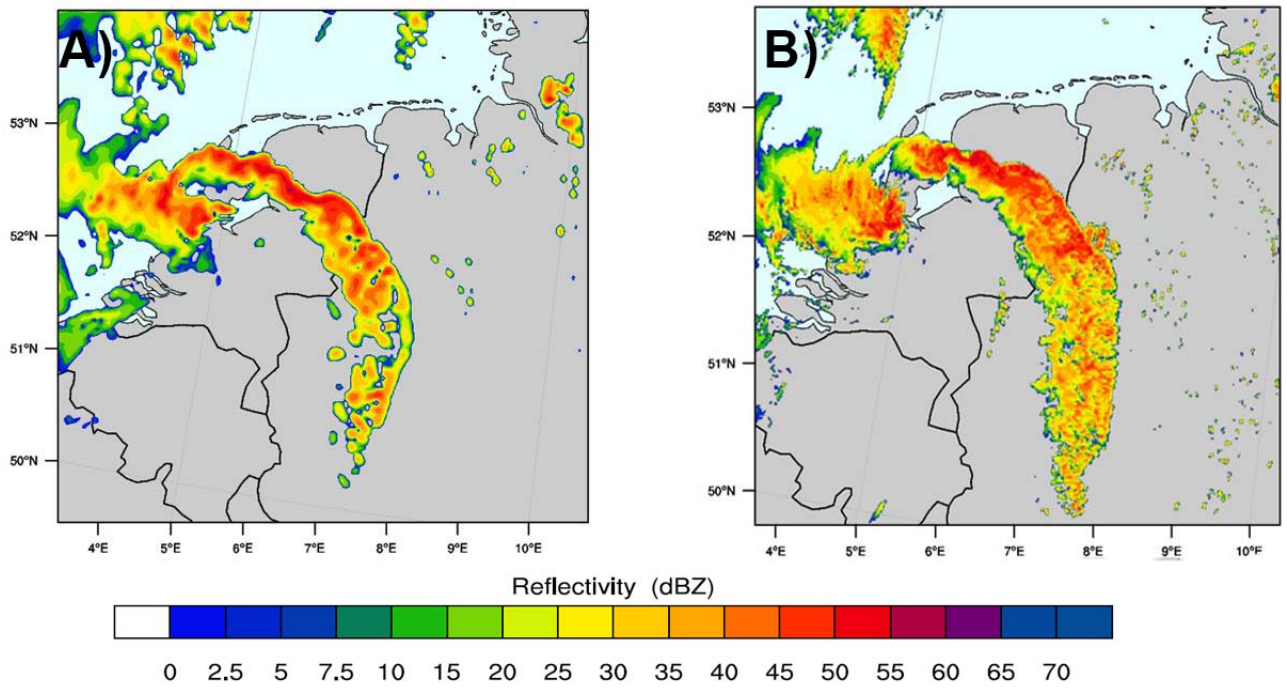

Figure 22: *Reflectivity (dBZ) at 12 UTC of the coarse resolution simulation (A) and de the fine resolution simulation (B)*

3.2.2 Cold pool

The cold pool (Figure 23) is a pocket of air near the surface which consists of air from a higher origin and therefore, it has lower temperatures than it surroundings. The Equivalent potential temperature (θ_e) gives a better insight in the origin of the air masses than the temperature. The coarse and fine resolution simulation having similar (θ_e). (Figure 23). At 11 UTC, the cold pool is located between the surface and 2km height in both simulations. They have te same minimum temperature (321K) as well. The shape of the cold pool is slightly different between the two simulations. Where the cold pool barely touches the surface, it touches the surface at several locations. Furthermore, the coarse resolution has a smooth border between the cold pool. The border of the cold pool is more heterogeneous and the shape is aciculated. Another interesting difference between the coarse and fine resolution is the large pocket of relatively warn air at 5.5°, this pocket of air has (θ_e) up to 339K, while in the smaller pocket of relatively warm air in the coarse resolution has a maximum (θ_e) of 337K. At the same location, at the surface the opposite exist, here the coarse resolution shows a larger pocket of warm than in the fine resolution simulation. Between 5.6-6.9°longitude, another difference can be found. In the coarse resolution a intrusion of colder air is present within in the relatively warm layer between 0-2.5km height.

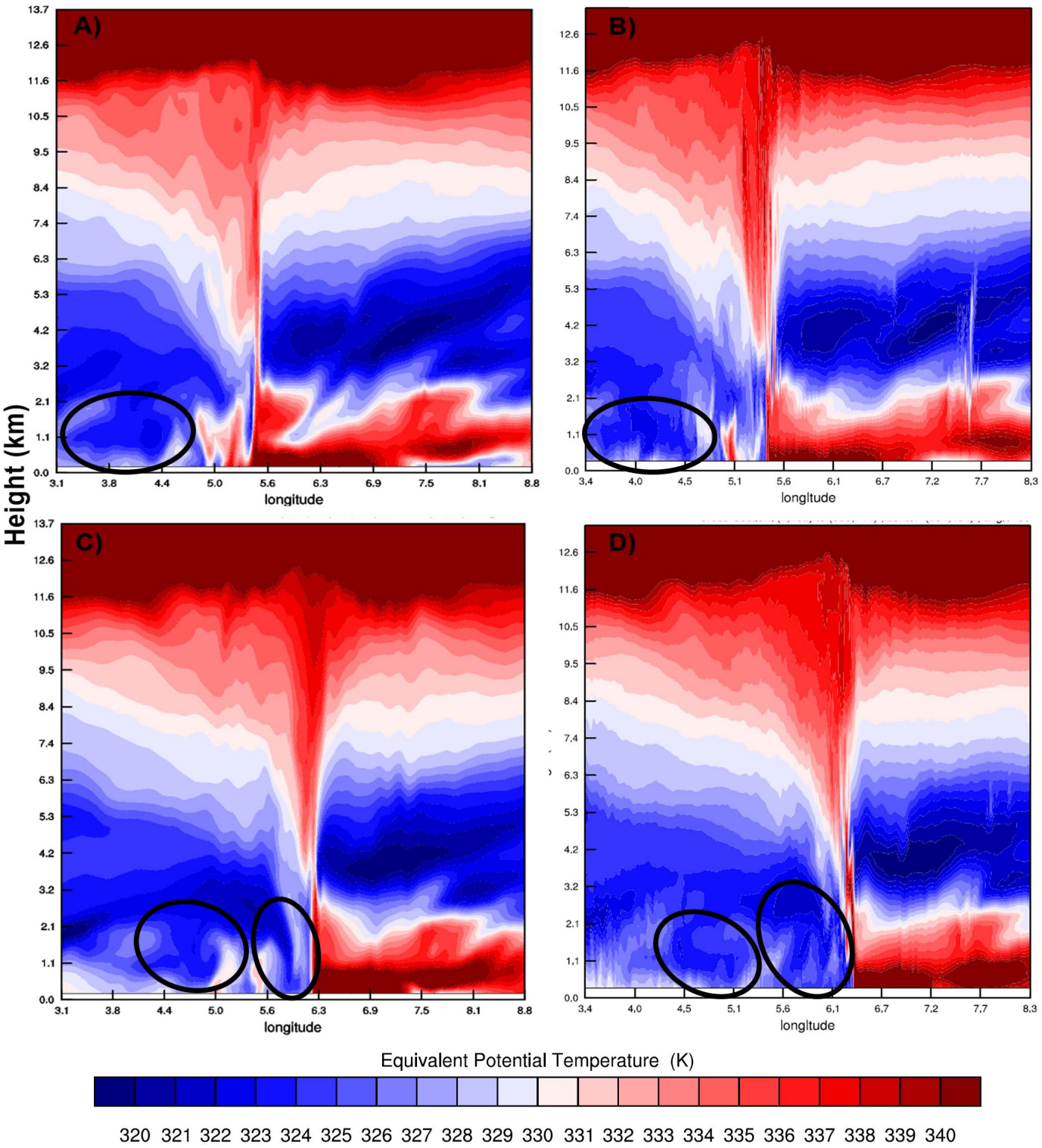

Figure 23: *The Equivalent potential temperature (K) at 11 UTC (A,B) and 12 UTC (C,D) of the coarse resolution simulation (A,C) and de the fine resolution simulation (B,D). The black circles show the location of the cold pool. The location of this cross-section can be found in Figure 24.*

A hour later the squall line has moved towards the north-east (Figure 23). Furthermore, a second cold pool can be found just behind the squall line. This secondary cold pool is more extensive in the fine resolution than in the coarse resolution. However the minimum (θ_e) (321k)

is for both and for both cold pools simulations as at 11 UTC. The shape of both cold pools in the fine resolutions remains aciculated. The warm intrusion which can be seen at 11UTC in the coarse resolution is almost completely gone.

On other time steps similar results can be found as described above. The fine and coarse resolution simulates similar (θ_e). However, there are some minor differences between them. For example the aciculated shape of the cold pool can be seen in all the time steps for the fine resolution. After all there is no clear difference between the location and the intensity of the cold pool between the coarse and fine resolution.

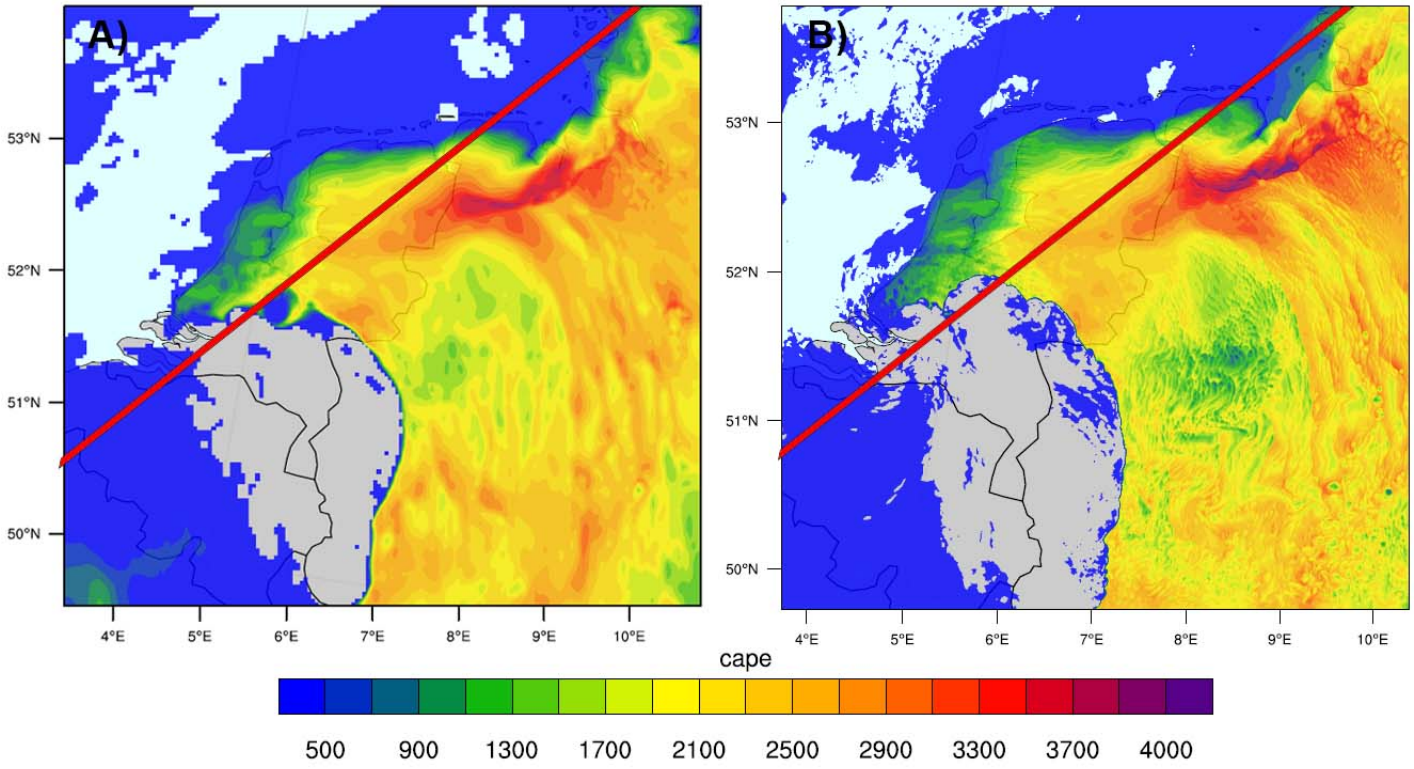

Figure 24: *CAPE (J/kg) of the coarse (A) and the fine resolution simulation (B). The red line shows the location of the cross-section in Figure 23.*

Although there is no clear difference found in the cold pool, the cold air intrusion in the coarse resolution at 11 UTC was investigated. Due to the this intrusion a thinner layer of warm air exists at the surface. Warm air below cold air means that the air is unstable at that location. Therefore, a lower instability could be expected at the location of the intrusion. However, the CAPE does not show a clear difference between the coarse and fine resolution simulation along the cross-section (Figure 24). Despite no clear difference can be found along the cross-section, some other differences can be found in the CAPE. Ahead of the squall line at 51.5°north shows a clear difference between the coarse and fine resolution. Where the fine resolution simulates a CAPE of only 650 J/kg, is the lowest CAPE of the coarse resolution 1300 J/kg. This means that the fine resolution is more unstable at this location. This could mean that the coarse resolution simulates a more intense squall line when it moves over that area. However, this is not visible in other variables (e.g precipitation)(not shown).

Wind speed could give an explanation of the cold intrusion, described in the previous paragraph. However at 11 UTC, no clear downward wind can be seen at the location of the cold air intrusion (18). Unfortunately we were not able to explain the cause of this cold air intrusion in the coarse simulation at 11 UTC.

3.3 RKW-theory

As described in Chapter 1, there are three stages in the development of a squall line. In an idealised case, locations of positive and negative vorticity can be found (Figure 2). In both coarse and fine resolution simulations, these locations are hardly to distinguish (Figure 25). There is a clear band of positive relative vorticity just behind the squall line reaching from 4.5km height to the surface in the coarse resolution simulation. However, in the fine resolution simulation this band is absent and a band of negative relative vorticity can been found. Due to the chaotic character of the results it is not possible make a good comparison between the RKW-theory and the vorticity data.

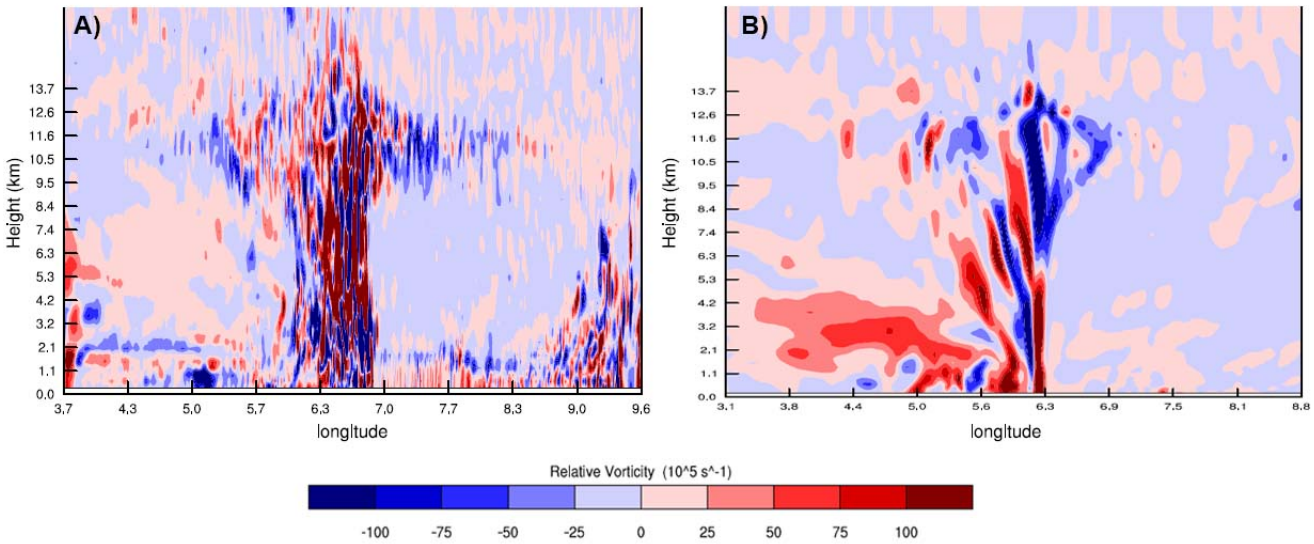

Figure 25: *Relative vorticity ($10^5 s^{-1}$) for the Coarse (A) en fine (B) resolution simulation. The location of this cross-section can be found in Figure 15.*

The results in Section 3.2.2 are suited to compare with the RKW-theory. Figure 23 shows similar patterns as in the RKW-theory (Rotunno et al. (1988), Figure 15). In both studies relatively warm can be found near the surface ahead of the squall line. Above this warm layer of air, a relatively cold layer of air can be found, which makes the air unstable ahead of the squall line. Between this cold layer and the tropopause, a relatively warm layer can be found. The lowest relatively warm layer of air ahead of the squall line is not present behind the squall line. Relatively cold air can be found near the surface up to the relatively warm layer near the tropopause.

4 Discussion and recommendations

This chapter will start with a short comparison between Uebel & Bott (2015) and our simulation. Although they used a different model, similar results could be expected because our coarse simulation had similar settings as their simulation. Additionally, some recommendations are given.

The majority of the results in the previous chapter are in accordance with the study performed by Uebel & Bott (2015). Both models had their problems with simulating this squall line event perfectly in accordance with the observations. In our simulations we had some problems with the orientation of the squall line and also the timing was not perfect. However the timing of the WRF simulations was better than the timing of the squall line in the simulation of Uebel & Bott (2015). Their surface pressure (Figure 11) is similar to our findings in surface pressure. Our simulation gives a pressure jump for the meso high and wake low of about 4 hPa and 6 hPa for the coarse and fine resolution, respectively, where in their simulation the jump is about 3 hPa. The pressure patterns in both studies are typical for the present weather situations (Haertel & Johnson, 2000). The passive tracer in both studies showed similar results too. However there are some differences. In our simulation relatively small amounts of the tracer penetrate trough the squall line. In their study (Uebel & Bott (2015), Figure 9), they found mixing ratios of 0.5 behind the squall line. It means that 50% of the air in that location consists of pre-squall line air. In our study we find values up to only 0.3. One of the reasons of this difference can be explained by the location of the cross-section and the intensity of the squall line. As they showed in their study, a small difference in location can give other results because of the heterogeneity in strength of the squall line (Uebel & Bott (2015), Figure 9 and 11). As our cross-section is not exactly at the same location this could lead to this difference in mixing ratio. Overall, our simulations give similar results with some minor differences. A part of these differences can be explained by the difference in analysis (e.g different location of cross-sections), but the main reason for the differences is the model: We used WRF, while they used the Consortium for Small-Scale Modelling (COSMO) model.

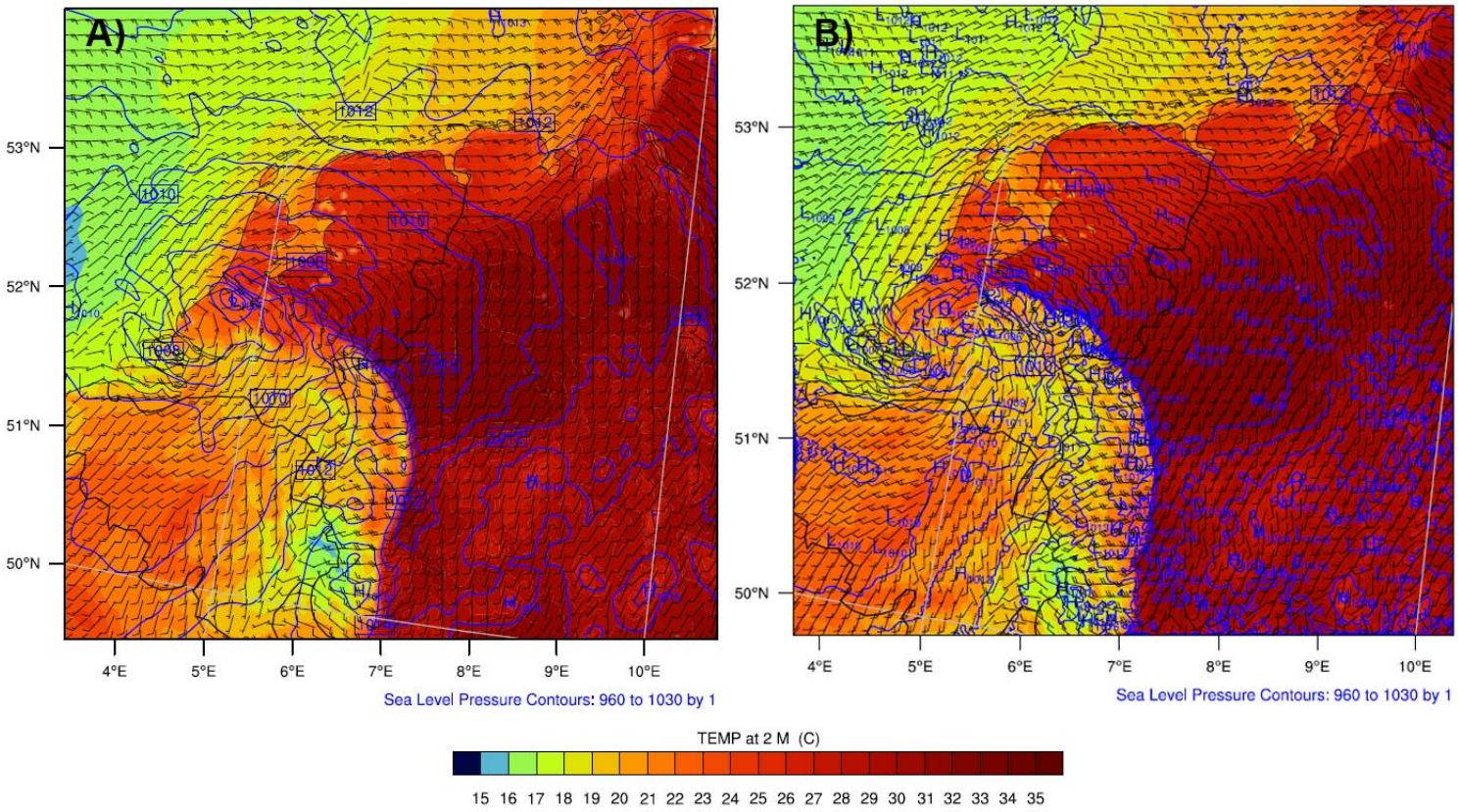

Figure 26: *Surface pressure (hPa) in contours, 2m-Temperature(°C) in colours and 10m wind barbs(m/s) at 11 UTC for the coarse (A) and fine (B) resolution simulation.*

The goal of this study was to get a better (quantitative) insight in the behaviour of the mixing of air within a squall line. Therefore it was not the goal to get the most realistic simulation in accordance with the observations. However, a realistic simulation could help to determine which resolution gave the most realistic output. In this study we compared the coarse resolution with the fine resolution. The coarse resolution was validated with observed variables (e.g. wind speed). However, this was not done for the fine resolution as the model had already some problems with simulating the perfect squall line in accordance with the observations. That is why it would not make sense to perform an extensive validation of the fine resolution simulation as well. Instead we made a comparison between the two simulations. Of course it would be interesting to determine if the fine resolution gives more realistic results. For this, the simulated squall line needs to be in accordance with the observations as much as possible.

In this study, the simulations were performed with use of a cumulus parametrization. However, for high resolution simulations, this is not always needed (e.g. Skamarock et al. (2008); Done et al. (2004); Weisman et al. (1997)). Other studies showed that in simulations with grid sizes less than 1km parametrization is still needed to solve deep convection (e.g. Bryan et al. (2003); Dawson et al. (2010); Petch et al. (2002)). Due to time limitation it was not possible to investigate if a simulation without parametrization gives more realistic results. However we found some signs that cumulus parametrization is not needed in the fine resolution; A relatively small part of the precipitation in the coarse simulation is parametrized, with a maximum of 2mm per 30 minutes (Figure 27). However, there is barely any precipitation parametrized in the fine resolutions simulation. This could be an indicator that, especially for the fine resolution, no cumulus parametrization is needed. For further research it would be very interesting to perform a sensitivity analysis of the cumulus parametrization on the air transport within a squall line at these high resolutions of 1km and higher to see whether these difference in precipitate are

caused by unjustified use of the cumulus parametrization.

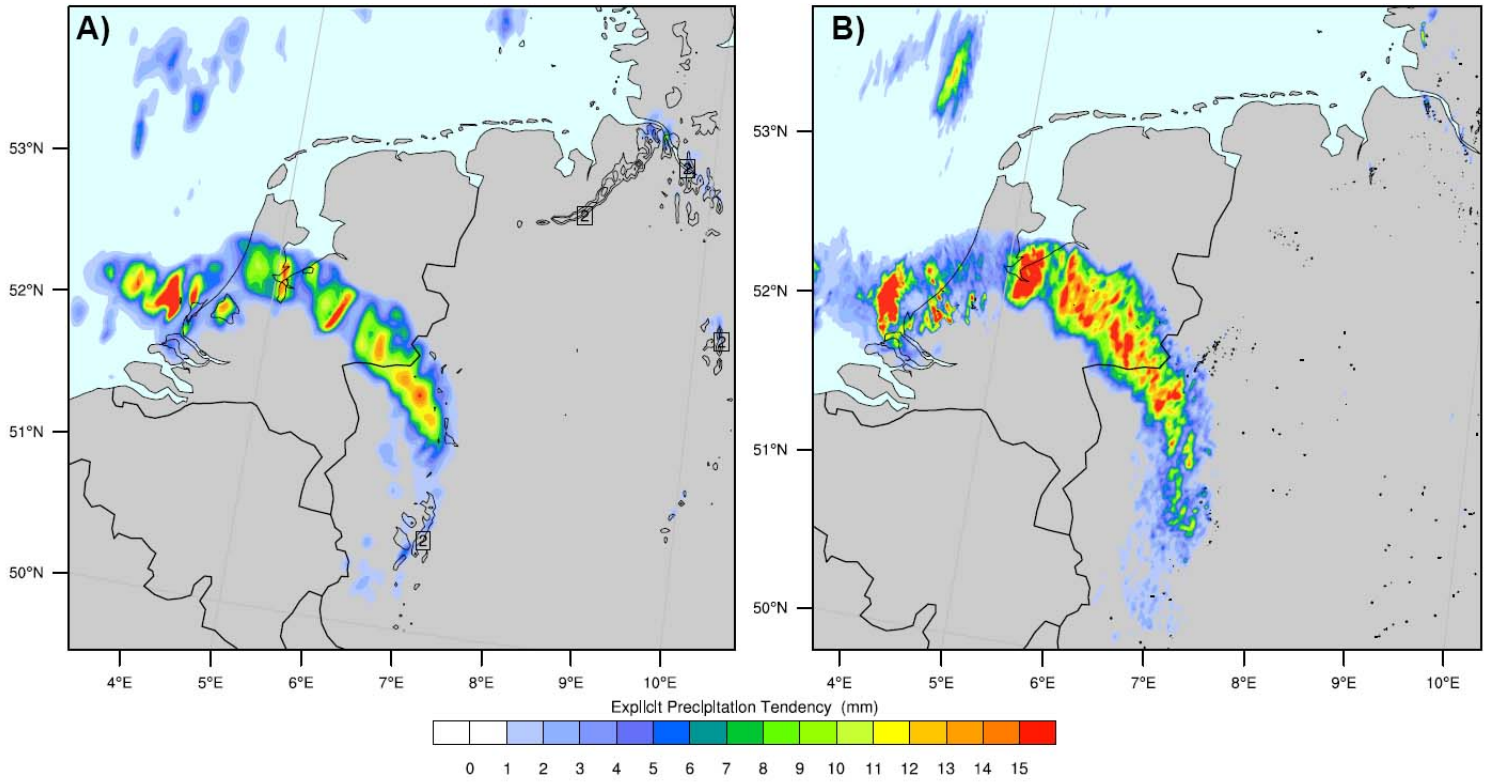

Figure 27: *Explicit Precipitation (colours) and parametrized precipitation (contour lines) in mm between 11.00-11.30 UTC in mm for the coarse (A) and fine (B) resolution simulation.*

5 Conclusions

In this study, we used the mesoscale Weather Research and Forecasting (WRF) model to simulate a squall line event (12th of July 2010). The aim of this study was to get a better (quantitative) insight into the behaviour of the mixing of air within a squall line. Therefore, the influences of horizontal resolution on the mixing of air within a squall line have been investigated. We performed two simulations with different horizontal resolutions, 3km and 0.6km called the coarse and fine resolutions simulation, respectively. Our results have been validated with the observations, which showed that the model did a reasonably good job in simulating a realistic squall line.

We first looked at the size of the updrafts and downdrafts. Our findings showed that the updrafts and downdrafts in the fine resolution are less horizontal extended and more heterogeneous than in the coarse resolution simulation. This heterogeneity creates an aciculated pattern in the amount of pre-squall line air that has been moved to other altitudes. In the fine resolutions, stronger vertical wind speeds can be observed than in the coarse resolution simulation. This caused more and stronger updraft and downdraft regions in the fine resolution simulation.

Next, we looked at the location and intensity of the cold pool within the squall line. The differences in cold pool are relatively small between the coarse and fine resolution. Both simulations show similar locations of the cold pool. The cold pool had the tendency to reach the surface more often in the coarse simulation than in the fine resolution simulation. There are no signs found for a difference in the intensity of the cold pool.

To conclude, an increase in horizontal resolution will lead to slightly more transport of air towards higher altitudes. However, the main pattern of mixing of air within a squall line remains the same. One should note that these results are specific for our chosen model settings. Different model setting, especially the choice of the spin-up time lead to different results.

References

Benjamin, T. B. (1968). Gravity currents and related phenomena. *Journal of Fluid Mechanics*, *31*(02), 209–248.

Bélair, S., & Mailhot, J. (2001). Impact of horizontal resolution on the numerical simulation of a midlatitude squall line: Implicit versus explicit condensation. *Monthly Weather Review*, *129*(9), 2362-2376. Retrieved from http://dx.doi.org/10.1175/1520-0493(2001)129<2362:IOHROT>2.0.CO;2 doi: 10.1175/1520-0493(2001)129<2362:IOHROT>2.0.CO;2

Brey, J., & Geer, E. (2000). *Glossary of weather, climate and ocean 2nd edition.*

Bryan, G. H., Knievel, J. C., & Parker, M. D. (2006). A multimodel assessment of rkw theory's relevance to squall-line characteristics. *Monthly Weather Review*, *134*(10), 2772-2792. Retrieved from http://dx.doi.org/10.1175/MWR3226.1 doi: 10.1175/MWR3226.1

Bryan, G. H., & Morrison, H. (2012). Sensitivity of a simulated squall line to horizontal resolution and parameterization of microphysics. *Monthly Weather Review*, *140*(1), 202–225.

Bryan, G. H., Wyngaard, J. C., & Fritsch, J. M. (2003). Resolution requirements for the simulation of deep moist convection. *Monthly Weather Review*, *131*(10), 2394-2416.

Carlson, T., & Ludlam, F. (1968). Conditions for the occurrence of severe local storms. *Tellus*, *20*(2), 203–226.

Dawson, D. T., Xue, M., Milbrandt, J. A., & Yau, M. (2010). Comparison of evaporation and cold pool development between single-moment and multimoment bulk microphysics schemes in idealized simulations of tornadic thunderstorms. *Monthly Weather Review*, *138*(4), 1152–1171.

de Rooy, W. C., Bechtold, P., Fröhlich, K., Hohenegger, C., Jonker, H., Mironov, D., ... Yano, J.-I. (2013). Entrainment and detrainment in cumulus convection: an overview. *Quarterly Journal of the Royal Meteorological Society*, *139*(670), 1–19. Retrieved from http://dx.doi.org/10.1002/qj.1959 doi: 10.1002/qj.1959

Done, J., Davis, C. A., & Weisman, M. (2004). The next generation of nwp: Explicit forecasts of convection using the weather research and forecasting (wrf) model. *Atmospheric Science Letters*, *5*(6), 110–117.

FMI. (n.d.). *Onvective cloud features in typical synoptic environments: The spanish plume - meteorological physical background.* Retrieved 28-10-2016, from http://rammb.cira.colostate.edu/wmovl/vrl/tutorials/satmanu-eumetsat/satmanu/cms/spl/backg

Fovell, R. G., & Ogura, Y. (1989). Effect of vertical wind shear on numerically simulated multicell storm structure. *Journal of the Atmospheric Sciences*, *46*(20), 3144-3176.

Haertel, P. T., & Johnson, R. H. (2000). The linear dynamics of squall line mesohighs and wake lows. *Journal of the Atmospheric Sciences*, *57*(1), 93-107. Retrieved from http://dx.doi.org/10.1175/1520-0469(2000)057<0093:TLDOSL>2.0.CO;2 doi: 10.1175/1520-0469(2000)057<0093:TLDOSL>2.0.CO;2

Hong, S.-Y., Lim, K.-S. S., Lee, Y.-H., Ha, J.-C., Kim, H.-W., Ham, S.-J., & Dudhia, J. (2010). Evaluation of the wrf double-moment 6-class microphysics scheme for precipitating convection. *Advances in Meteorology*, *2010*.

Houze, R. A. (1989). Observed structure of mesoscale convective systems and implications for large-scale heating. *Quarterly Journal of the Royal Meteorological Society*, *115*(487), 425–461.

Houze, R. A. (2004). Mesoscale convective systems. *Reviews of Geophysics*, *42*(4).

Hut, M. (2010, July). Tornado trekt spoor van vernieling in oost-nederland. *De Gelderlander*. Newspaper. Retrieved from `http://www.gelderlander.nl/achterhoek/tornado-trekt-spoor-van-vernieling-in-oost-nederland`

Johnson, R. H., & Hamilton, P. J. (1988). The relationship of surface pressure features to the precipitation and airflow structure of an intense midlatitude squall line. *Monthly Weather Review*, *116*(7), 1444-1473. doi: 10.1175/1520-0493(1988)116<1444:TROSPF>2.0.CO;2

Knmi: Maximum wind gust. (2010). Retrieved 2017-05-26, from `http://knmi.nl/nederland-nu/klimatologie/geografische-overzichten`

Kukkonen, J., Olsson, T., Schultz, D., Baklanov, A., Klein, T., Miranda, A., ... others (2012). A review of operational, regional-scale, chemical weather forecasting models in europe. *Atmospheric Chemistry and Physics*, *12*(1), 1–87.

Lebo, Z., & Morrison, H. (2015). Effects of horizontal and vertical grid spacing on mixing in simulated squall lines and implications for convective strength and structure. *Monthly Weather Review*, *143*(11), 4355–4375.

Litta, A., & Mohanty, U. (2008). Simulation of a severe thunderstorm event during the field experiment of storm programme 2006, using wrf-nmm model. *Current Science*, *95*(2), 204–215.

Markowski, P., & Richardson, Y. (2010). *Mesoscale meteorology in midlatitudes* (Vol. 2; Wiley-Blackwell, Ed.). John Wiley & Sons.

Petch, J., Brown, A., & Gray, M. (2002). The impact of horizontal resolution on the simulations of convective development over land. *Quarterly Journal of the Royal Meteorological Society*, *128*(584), 2031–2044.

Pimonsree, S., Ratnamhin, P., Vongruang, P., & Sumitsawan, S. (2016). Impacts of cumulus convective parameterization schemes on precipitation at grey-zone resolutions: A case study over complex terrain in upper northern thailand. *International Journal of Environmental Science and Development*, *7*(5), 359.

Rotunno, R., Klemp, J. B., & Weisman, M. L. (1988). A theory for strong, long-lived squall lines. *Journal of the Atmospheric Sciences*, *45*(3), 463-485.

Skamarock, W., et al. (2008). A description of the advanced research wrf version 3 (natl. cent. for atmos. res., boulder, co).

Stensrud, D. J., Coniglio, M. C., Davies-Jones, R. P., & Evans, J. S. (2005). Comments on a theory for strong long-lived squall lines revisited. *Journal of the Atmospheric Sciences*, *62*(8), 2989-2996. doi: 10.1175/JAS3514.1

Uebel, M., & Bott, A. (2015). Mesoscale air transport at a midlatitude squall line in europe–a numerical analysis. *Quarterly Journal of the Royal Meteorological Society*, *141*(693), 3297–3311.

University of wyoming. (2010). University of Wyoming. Retrieved from http://weather.uwyo.edu/upperair/sounding.html

Weisman, M. L., & Klemp, J. B. (1982). The dependence of numerically simulated convective storms on vertical wind shear and buoyancy. *Monthly Weather Review*, *110*(6), 504-520. Retrieved from http://dx.doi.org/10.1175/1520-0493(1982)110<0504:TDONSC>2.0.CO;2 doi: 10.1175/1520-0493(1982)110<0504:TDONSC>2.0.CO;2

Weisman, M. L., Klemp, J. B., & Rotunno, R. (1988). Structure and evolution of numerically simulated squall lines. *Journal of the Atmospheric Sciences*, *45*(14), 1990-2013. Retrieved from http://dx.doi.org/10.1175/1520-0469(1988)045<1990:SAEONS>2.0.CO;2 doi: 10.1175/1520-0469(1988)045<1990:SAEONS>2.0.CO;2

Weisman, M. L., & Rotunno, R. (2004). A theory for strong long-lived squall line revisited. *Journal of the Atmospheric Sciences*, *61*(4), 361-382.

Weisman, M. L., Skamarock, W. C., & Klemp, J. B. (1997). The resolution dependence of explicitly modeled convective systems. *Monthly Weather Review*, *125*(4), 527–548.

Wetterzentrale. (2010). Retrieved from http://old.wetterzentrale.de/topkarten/

Willmott, C. J. (1982). Some comments on the evaluation of model performance. *Bulletin of the American Meteorological Society*, *63*(11), 1309-1313.

Yu, X., & LEE, T.-Y. (2010). Role of convective parameterization in simulations of a convection band at grey-zone resolutions. *Tellus A*, *62*(5), 617–632.

Appendix A

RKW theory review

The RKW theory is based on several studies which were conducted earlier in the 1980's (e.g. Weisman & Klemp (1982) and Weisman et al. (1988)). The focus of these studies was on 3D simulations of a large amount of convective storms. The conclusion was that only an environmental shear profile is needed to form these convective storms. Based on these studies, the RKW theory states that for an optimal convective situation, the shear has to be approximately in balance with the surface cold pool. A surface cold pool is a small region with a lower temperature than its surroundings. The RKW theory also stated that lifting of the leading edge of a cold pool is an important process as this can trigger new convective cells to develop.

In 2004 this theory has been revisited by Weisman & Rotunno (2004). In this paper they were able to reconfirm that the balance between environmental shear and the intensity of the cold pool is important. They found that the deepest lifting can be found when these two are in balance. In another part of the paper of Weisman & Rotunno (2004), they looked to what extent the RKW theory is valid for a large variety of shears. This included not only shear in the lower atmosphere but also shear layers which were lifted. Besides they extended the simulations with a higher resolution and more measures to quantify the intensity of a squall line. In contrast with Rotunno et al. (1988) they found that longevity of squall lines can not be determined with this theory. In their simulations they found that all squall lines are long lived, this means that all of them lived for more than six hours. This finding is not completely new. Already in 1989 Fovell & Ogura (1989) found that their simulations lead to longer lived squall lines. Also in the case of less favourable balances between the cold pool and shear, their simulation lead to longer lived squall lines. On the contrary Rotunno et al. (1988) concluded that the balance between the shear and the strength of the cold pool is essential for the longevity of a squall line too, as stated by the RKW theory.

As a response to the revision of Weisman & Rotunno (2004), Stensrud et al. (2005) wrote a paper with criticism towards the findings of Weisman & Rotunno (2004). Stensrud et al. (2005) compared the simulation based on the RKW theory with real observations. They concluded that shear is an essential parameter for the development and structure of the squall line. However they argue whether the balance between the shear and the intensity of the cold pool is important for the development and structure for the squall line as the observations do not show this relationship. Besides that they found that not only the shear in the lower atmosphere as Weisman & Rotunno (2004) concluded but also the shear in the higher layers is important for the most long lived squall lines.

Bryan et al. (2006) evaluated the RKW theory as well. They conducted a multimodel assessment of the theory. They concluded that using different idealised simulations gives approximately the same results as in Weisman & Rotunno (2004). However the reader should be alert that in this study only a limited amount of environments has been tested and that this is not a complete validation of the RKW theory.

Spanish Plume

A Spanish Plume is a specific type of elevated mixed layer (EML) which is formed over Spain. This deep well-mixed layer in the lower atmosphere, develops at an elevated plateau, when a long period of warm and dry weather occurs. When in this period a low pressure system develops to the south of the United Kingdom it will cause a north ward flow from Spain towards the Benelux area. Due to the elevated plateau this air will not flow over the surface but at the height of the plateau (Figure 28). The EML will move over relatively moist and warm air that was already located over the West European continent. This makes the atmosphere highly unstable. However due to the two air masses often an inversion will be found on the top of the lowest air

mass. Such an air parcel needs to be triggered by something, e.g. by a front or by orographic effects, before convection takes place. Because this trigger is needed, it is hard to predict when and where convection will develop and create thunderstorms. However, if convection is able to start this can lead to severe storms because of the dry well-mixed air above it. Figure 29 shows an example sounding of an area with an EML. One can clearly see that there is an inversion around 900hPa. If an air parcel is able to overwin this inversion,it can freely rise up to 200hPa.

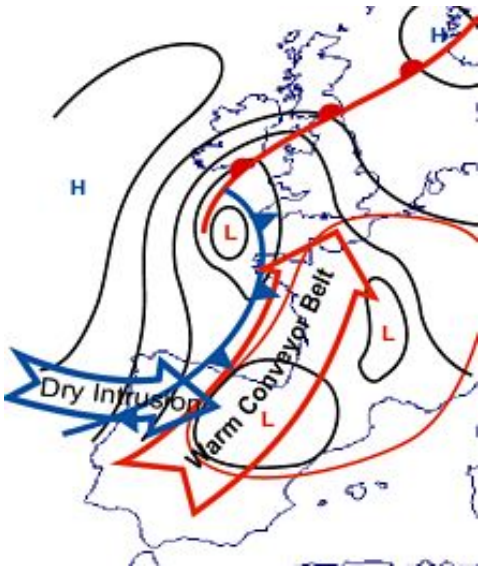

Figure 28: *Sounding of De Bilt, Netherlands at 12 July 2010 at 12UTC. The inversion due to the EML can be seen at the location of the arrow. (From:* University of Wyoming *(2010))*

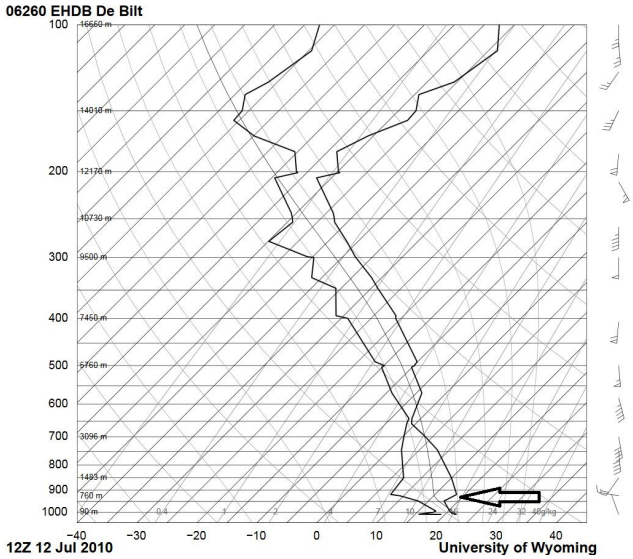

Figure 29: *Typical Spanish plume situation. Dry maritime air will move over Spain, blue arrow, while the warm and very dry air will move towards the north, red arrow. The low pressure system which causes this flow is also shown, south of the UK, with the accompanied warm and cold front. (From: (FMI, n.d.))*

Appendix B

In this Appendix, an explanation of how a passive tracer can be added to WRF version 3.7.1 is given. This section only consists of relevant (parts of) codes from the different WRF files. The complete scripts can be found on `https://gist.github.com/MikeBudde` .

Initialisation of the tracer

To initialise a passive tracer it is needed to modify a couple of WRF files. To start with, one line has to be added in the file namelist.input (WRF/WRFV3/run/). Under the section of dynamics, this line has to be added:

namelist.input

```
tracer_opt = 2, 2, 2
```

In this case the simulation is performed with three nested domains, so it is important set tracer_opt to 2 for all the three domains. After adding this line, some modifications in the Registry.EM file (WRF/WRF/Registry/) have to be made. The original tracer options can be replaced by the tracers of interest. In this case we defined three different passive tracers, tr_low, tr_mid and tr_high.

Registry.EM (Line 41-46)

```
1)        state   real    -          ikjftb  tracer        1         -     -    -
2)        state   real    tr_low     ikjftb  tracer        1         -     irhusdf=(bdy_interp:dt)    "tr_low"...
               "tr_low"     "Dimensionless"
2)        state   real    tr_mid     ikjftb  tracer        1         -     irhusdf=(bdy_interp:dt)    "tr_mid"...
               "tr_mid"     "Dimensionless"
4)        state   real    tr_high    ikjftb  tracer        1         -     irhusdf=(bdy_interp:dt)    "tr_high"...
               "tr_high"    "Dimensionless"
5)
6)        package tracer_test1 tracer_opt==2 - tracer:tr_low,tr_mid,tr_high}
```

By defining more tracers it is possible to release more tracers simultaneously during the simulation. Important hereby is to change line 46 too. After making these changes it is good to recompile WRF to check whether or not errors have been made. When the code is exactly the same as the code used in this case, but WRF still gives errors, than in that WRF version it is not possible to remove the original tracers. To solve this problem the lines given in the code of Appendix have to be added to the original tracers instead of replacing them. This causes a larger WRF-output file, but for the moment that is the only solution.

When WRF is compiled successfully, module_initialize_real.F (WRF/WRFV3/dyn_em) can be edited. In this file the exact details (e.g. Location and height) of the tracer will be added. The next piece of code has to be added around line 3372:

Module.initialize.real.F (Line 3372-3383)

```
1)        IF (config_flags%tracer_opt .eq. 2) THEN
2)                DO j = (jde + jds)/2 - 4, (jde + jds)/2 + 4, 1
3)                        DO i = (ide + ids)/2 - 4, (ide + ids)/2 + 4, 1
4)                                IF ( its .LE. i .and. ite .GE. i .and. jts .LE. j .and. jte .GE. j ) THEN
5)                                        tracer(i, 1, j, P_tr

_low) = 0.
6)                                        tracer(i, 1, j, P_tr_mid) = 0.
7)                                        tracer(i, 1, j, P_tr_high) = 0.
8)                                END IF
9)                        END DO
10)                END DO
11)        END IF
```

The two do loops create a square of 8x8 grid points in the middle of the domain. In this case there is a concentration of 0 for all the three tracers. So it does not matter where the tracer will be initialised. If the tracer needs to be initialised at the start of the simulation, these zeros can be replaced by an value. And the do loop can be replaced to determine a different location of initialisation. The IF-statement above is only needed when the simulation uses parallel calculations. After these changes it is good to re-compile WRF again.

The last file that has to be changed is the solve_em.F (WRF/WRFV3/dyn_em). First addition that is needed:

solve_em.F (Line 181)

```
integer :: xread(1:177,1:198), yread(1:198), row, col
```

These line initialises the variables 'xread', 'yread', 'row', 'col'. The variables are needed later on as can be seen in the next piece of code:

solve_em.F (Line 274-332)

```
1) open (unit = 10, file = "Tracer_conditional.txt")
2) READ (10,*) ((xread(col,row),col=1,174),row=1,168)
3) CLOSE(10)
4)
5) !2160 = 12h, 1980=11h
6) IF ( config_flags%tracer_opt == 2 ) THEN
7)        IF (grid%id == 2 ) THEN
8)                IF ( grid%itimestep == 1980 ) THEN
9)                        DO i = 0, 173
10)                               DO j = 0 ,167
11)                                       IF (ips .LE. i .and. ipe .GE. i .and. jps .LE. j .and. jpe .GE. j ) THEN
12)                                              IF (xread(i,j) == 1 ) THEN
13)                                                      DO k = 1, 17
14)                                                              tracer(i,k,j,P_tr_low) = 1.
15)                                                      END DO
16)                                              END IF
17)                                      END IF
18)                               END DO
19)                       END DO
20)               END IF
21)        END IF
22)END IF
23)
24) !2160 = 12h, 1980=11h
25) IF ( config_flags%tracer_opt == 2 ) THEN
27)        IF (grid%id == 2 ) THEN
28)                IF ( grid%itimestep == 1980 ) THEN
29)                        DO i = 0, 173
30)                               DO j = 0 ,167
31)                                       IF (ips .LE. i .and. ipe .GE. i .and. jps .LE. j .and. jpe .GE. j ) THEN
32)                                              IF (xread(i,j) == 1 ) THEN
33)                                                      DO k = 17, 14
34)                                                              tracer(i,k,j,P_tr_mid) = 1.
35)                                                      END DO
36)                                              END IF
37)                                      END IF
38)                               END DO
39)                       END DO
40)               END IF
41)        END IF
42)END IF
43)
44) !2160 = 12h, 1980=11h
45) IF ( config_flags%tracer_opt == 2 ) THEN
46)        IF (grid%id == 2 ) THEN
47)                IF ( grid%itimestep == 1980 ) THEN
48)                        DO i = 0, 173
49)                               DO j = 0 ,167
50)                                       IF (ips .LE. i .and. ipe .GE. i .and. jps .LE. j .and. jpe .GE. j ) THEN
51)                                              IF (xread(i,j) == 1 ) THEN
52)                                                      DO k = 24, 28
53)                                                              tracer(i,k,j,P_tr_high) = 1.
54)                                                      END DO
55)                                              END IF
56)                                      END IF
57)                               END DO
58)                       END DO
59)               END IF
60)        END IF
61)END IF
```

The first lines will import a file with zeros and ones for every grid point This file determines the locations were the tracer will be released. After importing these location, a large if statement is needed to check if every requirement is satisfied. It check if it is in the right domain (line 7), if the required time step has been reached (line 8). The do-loops are a loop over all the grid points

in that domain. After the do-loop, a new if statement can be found, this one is similar to the if statement in the Module.initialize.real.F-file and is only needed in case of parallel calculations. The if statement hereafter, checks whether the important file has a '1' or a '0' zero for that specific grid point. If it equals one, it means that the tracer has to be released in the grid point in all the eta levels specified in the do loop after this, if it equals zero, it means that nothing has to be done for this grid point. Lines 24-42 and lines 44-61 are similar to lines 5-22, the only difference is the height that the tracer will be released.

The previous code is quite extensive and can probably be reduced to the next piece of code. However this has not been tested yet!

solve_em.F (Line 274-332)

```
1) open (unit = 10, file = "Tracer_conditional.txt")
2) READ (10,*) ((xread(col,row),col=1,174),row=1,168)
3) CLOSE(10)
4)
5) IF ( config_flags%tracer_opt == 2 ) THEN
6)        IF (grid%id == 2 ) THEN
7)                IF ( grid%itimestep == 1980 ) THEN
8)                        DO i = 0, 173
9)                                DO j = 0 ,167
10)                                       IF (ips .LE. i .and. ipe .GE. i .and. jps .LE. j .and. jpe .GE. j ) THEN
11)                                              IF (xread(i,j) == 1 ) THEN
12)                                                     DO k = 1, 17
13)                                                             tracer(i,k,j,P_tr_low) = 1.
14)                                                     END DO
15)                                                     DO k = 17, 14
16)                                                             tracer(i,k,j,P_tr_mid) = 1.
17)                                                     END DO
18)                                                     DO k = 24, 28
19)                                                             tracer(i,k,j,P_tr_high) = 1.
20)                                                     END DO
21)                                              END IF
22)                                       END IF
23)                                END DO
24)                        END DO
25)                END IF
26)        END IF
27)END IF
```